7-1-1998

Analysis of potential base-pairs between 16S and 23S ribosomel RNA in Escherichia coli.

Bruce Carden

Analysis of Potential Base-Pairs Between 16S and 23S Ribosomal RNA in *Escherichia coli*

A Thesis

Presented to the

Department of Biology

and the

Faculty of the Graduate College

University of Nebraska

In Partial Fulfillment

of the Requirements for the Degree

Master of Arts

University of Nebraska at Omaha

by

Bruce M. Carden

July 1998

THESIS ACCEPTANCE

Acceptance for the faculty of the Graduate College,
University of Nebraska, in partial fulfillment of the
requirements for the degree Master of Arts,
University of Nebraska at Omaha.

Committee

Name	Department/School
A. Thomas Weber	Biology
Richard B. Linnett	Chemistry
John C. Mueller	Biology

Chairperson William C Tapprich

Date July 13, 1998

ABSTRACT

Each ribosome in *E. coli* is composed of two associated subunits, the 30*S* small subunit and the 50*S* large subunit, forming the translationally competent 70*S* ribosome. Ribosomal subunit association is a critical feature of all stages of translation. One proposal for subunit association involves rRNA-rRNA interactions between the 790 loop in 16*S* rRNA and the 2750 loop in 23*S* rRNA. Each of these sequences are highly conserved, and more intriguingly have the potential to form Watson-Crick base-pairs with each other. The objectives of this study were to detail the role of the 2750 loop in subunit association and test the hypothesis that these regions base-pair during subunit association. These objectives were explored using site-directed mutagenesis. Single mutations were constructed at position 2755 of 23*S* rRNA and double mutants were constructed between positions 791 of 16*S* rRNA and 2755 of 23*S* rRNA.

The results of this study indicate that the 790 and 2750 loops are not interacting by simple Watson-Crick base-pairing. The single mutations at position 2755 have little, or no, obvious effect on cell growth or subunit association (in the 7-deletion strain). However, slight differences in DMS modification within the 2750 loop indicate that the single mutations most likely confer a conformational change within the 2750 loop, but do not induce a change across the subunit in the 790 loop. The viable double mutants in the 7-deletion strain have much greater effects on ribosome structure, subunit association and cell growth. Each of the double mutants have very deleterious effects on subunit association as well as cell growth. The most prominent effect of these mutations is the effect on the structure of the 790 and 2750 loops in 70*S* ribosomes. The introduction of the 2755G and 2755U mutations rescue lethal 791A and 791U single mutants. It is proposed that the mutations at position 2755 allow the 2750 loop to interact with the 790 loop mutant at position 791. This interaction involves the mutant 2750 loop conferring a conformational

change across the ribosomal subunits to the mutant 790 loop, converting the 790 loop to a more exposed structure allowing for the improved function of the ribosomes.

Acknowledgements

I would like to thank Dr. William Tapprich for his guidance and support throughout my career in his laboratory. Dr. John Mullican has been greatly appreciated for his helpful suggestions and discussions. To others in the laboratory, especially Shelton Bradrick, I extend my thanks and best wishes. I would also like to thank my committee members, Dr. A. Thomas Weber and Dr. Richard Lomneth for assistance during this project. I am grateful to Dr. Albert Dahlberg and my colleaugues in the lab at Brown University for insight, help, discussions and support. Finally, I would like to thank my family and friends for their continued patience and support, especially Damon who is my inspiration.

Table of Contents

List of Figures

List of Tables

Chapter 1. Introduction

Gene expression is a complex cellular process involving many macromolecules, including DNA, RNA, and proteins. Of central importance are the RNA molecules such as messenger RNA (mRNA), transfer RNA (tRNA) and ribosomal RNA (rRNA) that participate directly in the gene expression mechanism. The rRNA class of RNA molecules, with the help of tRNAs, is required for decoding genetic information provided by mRNAs into functional proteins. This enzymatic process is carried out by the ribosome, in which the rRNA molecules provide the primary structural and catalytic activities.

In *Escherichia coli* (*E. coli*) cells, three rRNA molecules, 5*S* rRNA, 16*S* rRNA, and 23*S* rRNA, associate with 54 ribosomal proteins to form the multienzyme ribosomal complex. Ribosomes are unique enzymes, in part because they are composed of two very distinct subunits, a 30*S* small subunit and a 50*S* large subunit. The 30*S* subunit is composed of the 1542 nucleotide (nt) 16*S* rRNA (Figure 1) and 21 ribosomal proteins (S1-S21). The 50*S* subunit contains the 120 nt 5*S* rRNA, the 2904 nt 23*S* rRNA (Figure 2a, 2b) and 33 ribosomal proteins (L1-L36). The 30*S* and 50*S* subunits interact and associate to form 70*S* ribosomes (Figure 3).

Processes of Protein Synthesis

The process of protein synthesis involves the translation of mRNA into protein. This process occurs in three distinct stages; initiation, elongation and termination. Translation initiation requires three accessory proteins, initiation factors 1, 2 and 3 (IF1, IF2 and IF3), that interact with free 30*S* subunits. IF1 and IF3 dissociate 70*S* ribosomes and shield sites important for the elongation cycle. This ensures that mRNA and initiatior tRNA can interact efficiently with the free 30*S* subunit. IF2, coupled to a molecule of

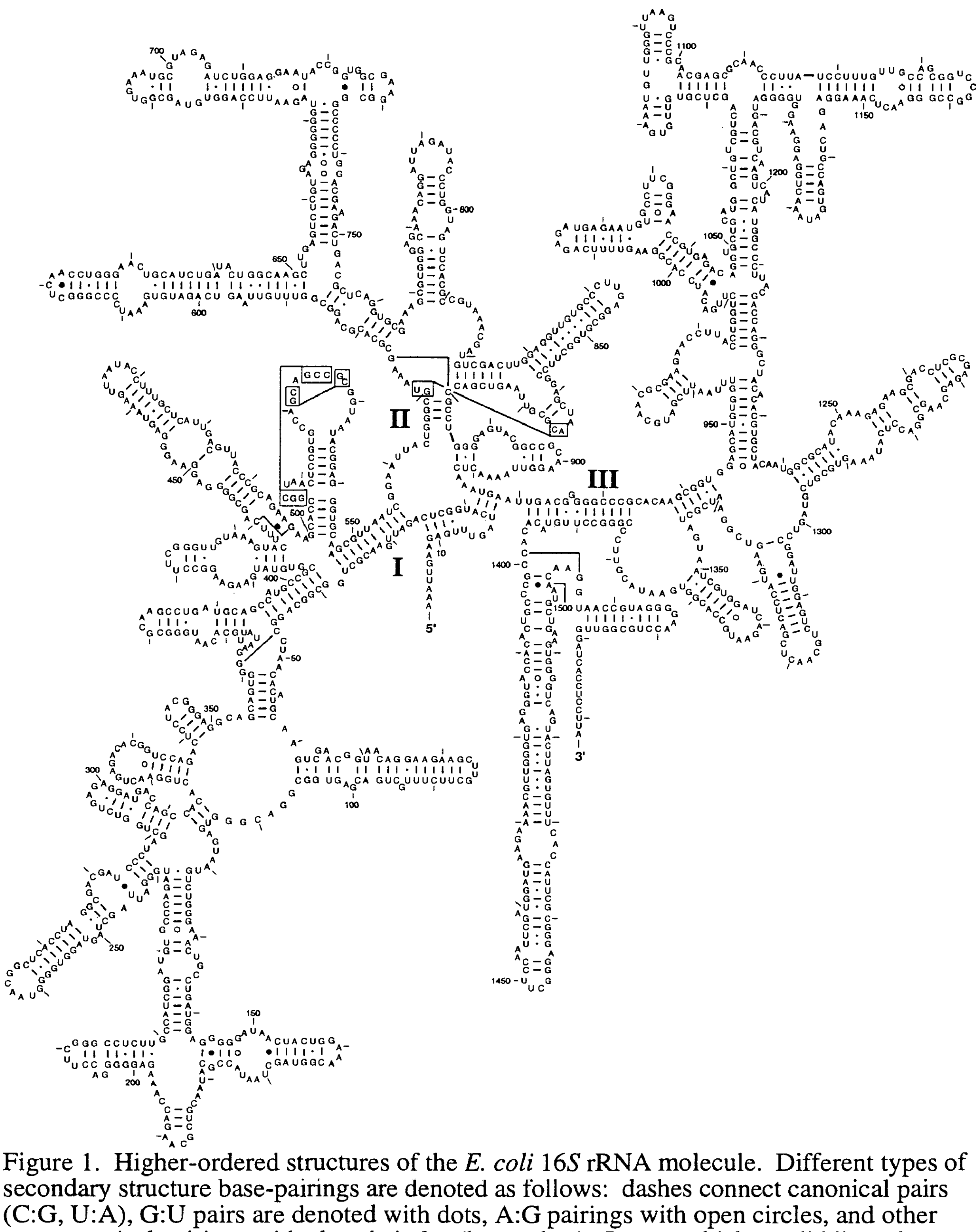

Figure 1. Higher-ordered structures of the *E. coli* 16*S* rRNA molecule. Different types of secondary structure base-pairings are denoted as follows: dashes connect canonical pairs (C:G, U:A), G:U pairs are denoted with dots, A:G pairings with open circles, and other non-canonical pairings with closed circles (larger dots). Longer, thicker solid lines denote tertiary interactions. Figure reproduced from reference (Gutell, R.R., 1994).

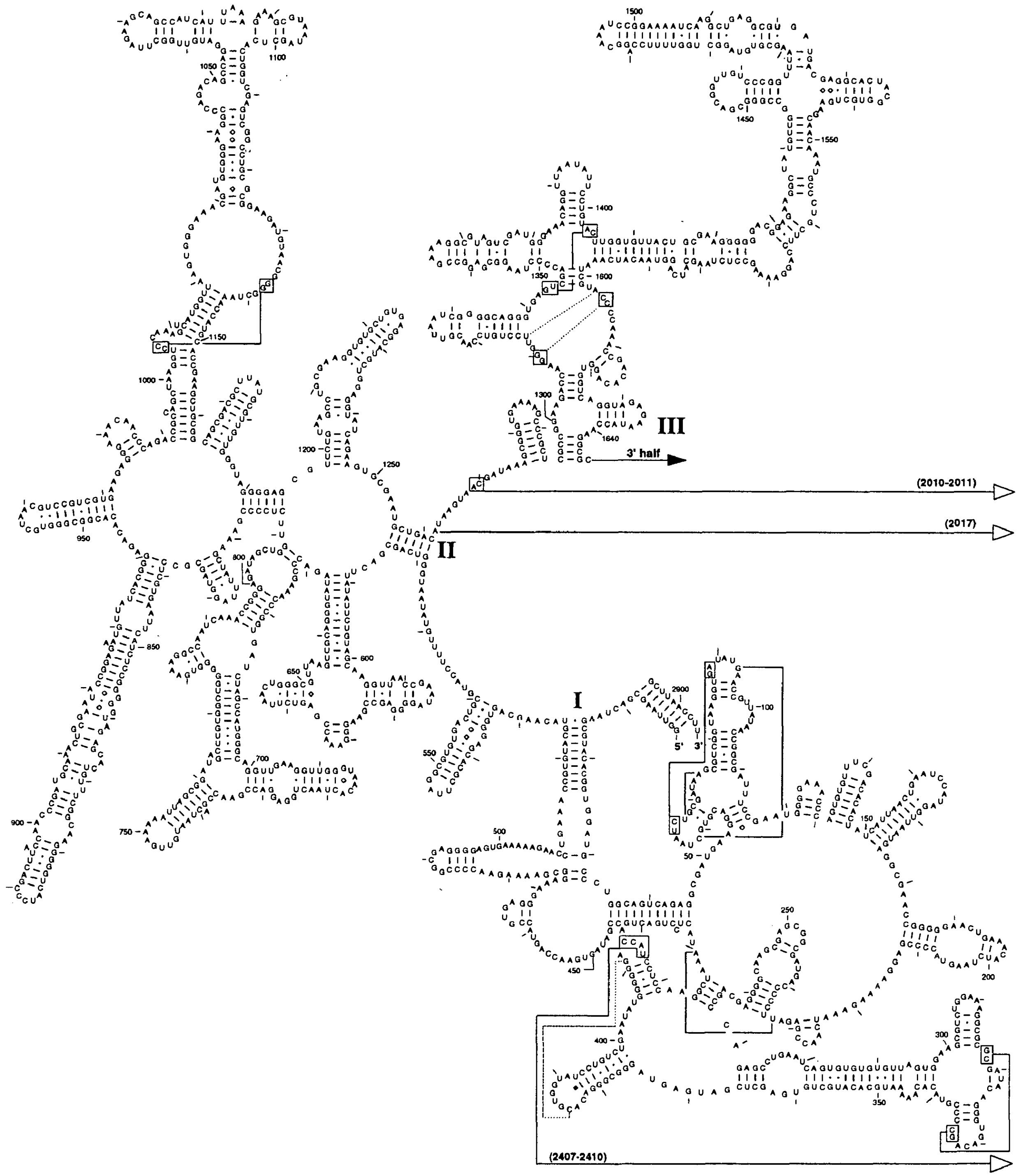

Figure 2a. The 5' half of the 23*S* rRNA secondary structure of *E. coli*. Pairings are as described in Figure 1 legend. Figure reproduced from reference (Gutell, R.R., 1994).

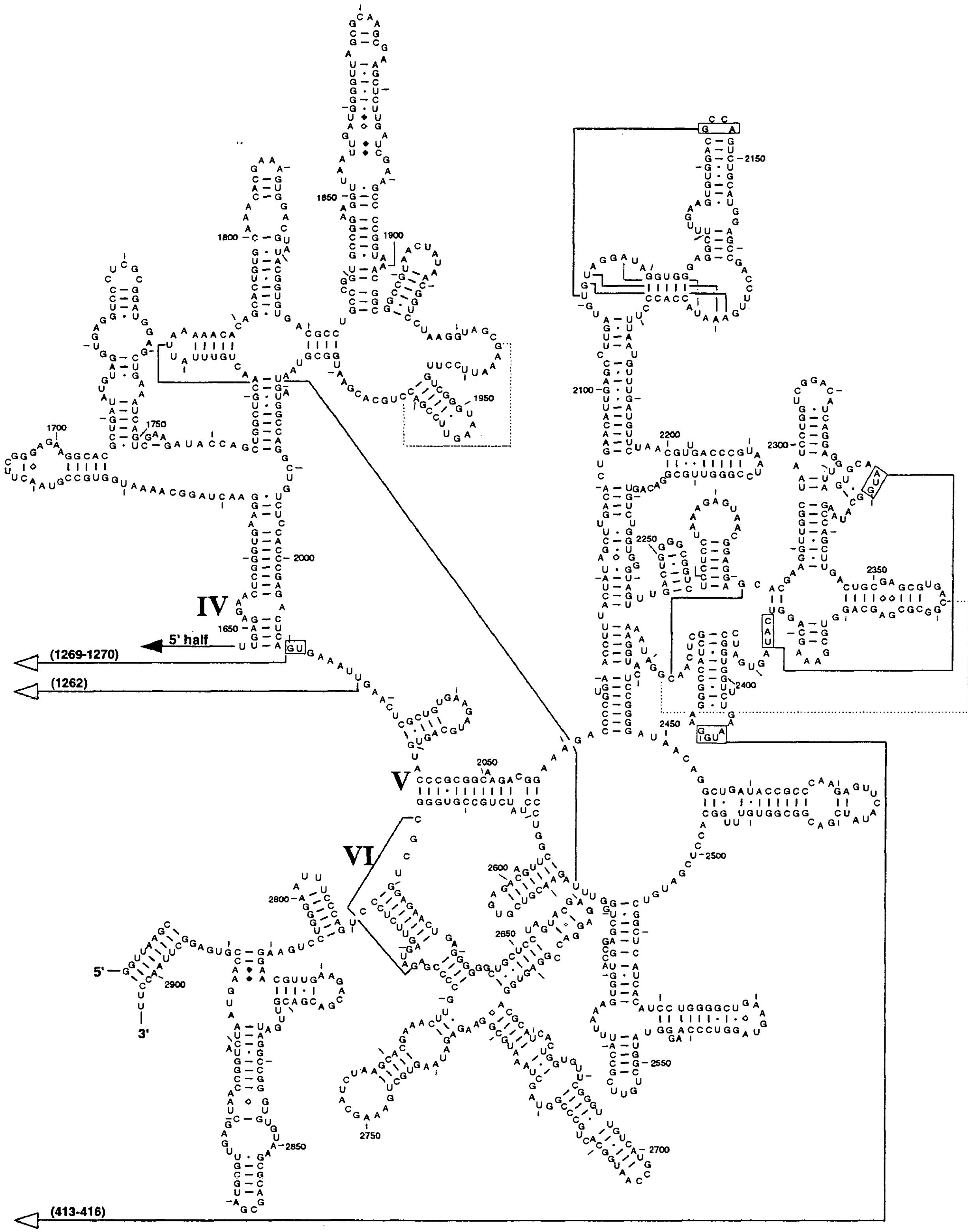

Figure 2b. The 3' half of the 23*S* rRNA secondary structure of *E. coli*. Pairings are as described in Figure 1 legend. Figure reproduced from reference (Gutell, R.R., 1994).

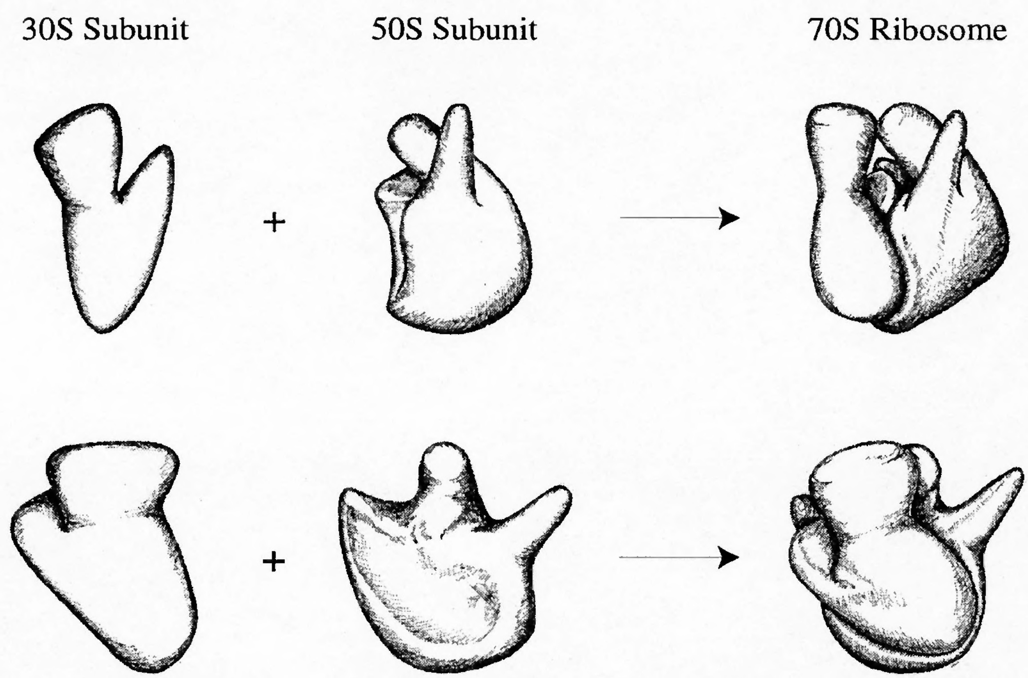

Figure 3. A three-dimensional model of the 30S, 50S and 70S ribosomal particles from *E. Coli.*

GTP, is the last initiaton factor to bind. IF2 binds to the 30*S* subunit along with fMet-tRNA, placing this initiator tRNA into the 30*S* peptidyl site (P-site). At approximately the same time that the IF2-fMet-tRNA complex is bound, the Shine-Dalgarno sequence of mRNA pairs to nucleotides 1535-1540 (*E. coli* numbering; 5' CCUCCU 3') at the 3' end of the 16*S* rRNA. Once the mRNA and initiator tRNA are properly placed on the 30*S* subunit, IF3 is released, forming a 30*S* initiation complex that has a high affinity for 50*S* subunits. Once the 50*S* subunit associates, the mRNA AUG initiator codon with its bound $tRNA^{fMet}$ aligns with the P-site of the 50*S* subunit. At this point, the GTP carried by IF2 is hydrolyzed and IF2-GDP, P_i, and IF1 are all released. The 70*S* initiation complex is now formed and the elongation process commences.

During elongation, the mRNA codon corresponding to the next amino acid to be incorporated is aligned with the aminoacyl site (A-site) of the 70*S* complex. The appropriate aminoacyl-tRNA is decoded into the A-site by a ternary complex composed of elongation factor Tu (EF-Tu), and GTP. Once the aminoacyl-tRNA is positioned in the A-site, GTP is hydrolyzed and EF-Tu-GDP is released. The formyl methionine bound to the tRNA in the P-site (or the nascent polypeptide chain in subsequent elongation cycles) is then transferred to the amino group of the amino acid bound to the tRNA occupying the A-site in a process called peptidyl transfer. Long thought to be catalyzed by ribosomal proteins, the peptidyl transferase acitivity of the ribosome is likely to be an enzymatic property of 23*S* rRNA (Noller and Zimniac, 1992). Following formation of the peptide bond, translocation moves newly formed peptidyl tRNA from the A-site to the P-site and the uncharged tRNA from the P-site to the A-site. Translocation requires elongation factor G (EF-G) and again is coupled to GTP hydrolysis.

Termination of translation occurs when a mRNA stop codon is translocated into the A-site. Three release factor proteins, RF1, RF2, and RF3 function in the release of the polypeptide from the ribosome. When a stop codon occupies the A-site, either RF1 or RF2 binds to the ribosome (depending upon the identity of the stop codon) followed by RF3, which is believed to aid in the peptide release process via GTP hydrolysis. Using the peptidyltransferase activity, the C-terminal amino acid is transferred from the peptidyl-tRNA to a water molecule, releasing the polypeptide from the ribosome. Translation is complete following the release of RF1, RF2, RF3 and GDP. The 70*S* complex then dissociates into free 30*S* and 50*S* subunits that re-enter the initiation cycle.

Subunit Association

The process of ribosomal subunit association is a critical feature of all stages of translation. This process plays its first role during the transition from initiation to elongation with the binding of the 50*S* subunit to the 30*S* initiation complex (Wilson & Noller, 1998a). Dynamic changes during elongation (Wilson & Noller, 1998a), including translocation (Wilson & Noller, 1998b) are dependent on the association of the two subunits and these movements of the associated subunits may provide an explanation for the two-subunit structure of the ribosome (Wilson & Noller, 1998b; Bretscher, 1968; Spririn, 1968). Finally, dissociation of the subunits following termination is an absolute necessity to allow for a new round of translation involving the formation of the 30*S* initiation complex followed by the transition from initiation to elongation as mentioned above.

Most studies of the association process have detailed the 30*S* subunit components that participate in subunit-subunit interactions. To this point, very little knowlegde has been generated concerning the role of the large ribosomal subunit in the association process. Two base-paired regions within the penultimate stem (nt 1409-1491) of 16*S* rRNA have been implicated in the process of subunit association (Rottman et al., 1988; Firpo & Dahlberg, 1998). Several single-stranded regions of 16*S* rRNA and two single stranded regions of 23*S* rRNA have also been implicated in this process. These regions include the 700 region (Chapman & Noller, 1977; Herr et al., 1979), the 790 loop in the central domain (Herr et al., 1979; Tapprich & Hill, 1986; Tapprich et al., 1989), and nucleotides 1530 and 1531 in the 3' minor domain of 16*S* rRNA (Firpo et al., 1996). The single stranded regions of 23S rRNA that have been implicated in subunit association are the 2750 loop in domain VI and nucleotides 2306-2313 in domain V (Hill et al., 1988).

The 790 Loop

In the process of subunit association, the most notable region of 16*S* rRNA is a hairpin loop in the central domain of 16*S* rRNA surrounding position 790. The 790 loop is a nine nucleotide single-stranded loop encompassing positions 787-795 in *E. coli* 16*S* rRNA (Figure 1). Six of the nine nucleotides within the loop are universally conserved, with the remaining two positions being strongly conserved (Gutell et al., 1994). The 790 loop has been implicated in subunit association (Herr et al., 1979; Tapprich &Hill, 1986; Tapprich et al., 1989), IF3 binding (Muralikrishna & Wickstrom, 1989; Tapprich et al., 1989), and tRNA binding (Moazed & Noller, 1986). This loop has been shown to be located on the surface of the 30*S* subunit and at the interface between 30S and 50S subunits (Chapman & Noller, 1977; Tapprich & Hill, 1986).

A study by Staplin (1995) showed that mutation of 790A to 790C or 790U, greatly decreased the affinity of mutant 30*S* subunits for wild-type 50*S* subunits. Interestingly, in the same study, the mutation of 790A to 790G resulted in mutant 30*S* subunits acquiring a higher affinity for wild-type 50*S* subunits (Staplin, 1995). Santer et al. (1990) demonstrated that the mutation of position 792A to 792C, G or U resulted in decreased affinity of mutant 30*S* subunits for wild-type 50*S* subunits.

The mutation of universally conserved 791G to 791A showed a significant deficiency in subunit association, as well as deficiencies in growth, IF3 binding and *in vitro* translation of polyU mRNA (Tapprich et al., 1989). Additionally, an oligonucleotide probe bound to nucleotides 787-795 of the 790 loop greatly inhibited binding of 30*S* subunits with wild-type 50*S* subunits (Tapprich & Hill, 1986).

Subunit association was prevented with several site-directed double mutants between positions 787 and 795 which result in stable base-pairs between these two positions (Lee et al., 1996). It is proposed that these mutations indirectly affected ribosome function by altering the structure of the 790 loop (Lee et al., 1996).

Modification of nucleotides using chemical modifying reagents has been used to explore the structure of the region in and around the 790 loop (Chapman & Noller, 1977; Herr, Chapman & Noller, 1979; Moazed & Noller, 1986; Moazed & Noller, 1990). Positions 790A and 795C are protected from chemical modification by tRNA bound to the P-site or by bound 50*S* subunits (Moazed & Noller, 1990). When 50*S* subunits were bound to 30*S* subunits 793U became protected from modification and this protection was strengthened by tRNA binding to both the A and P-sites (Moazed & Noller, 1990). Position 791G has been shown to be protected from modification in 70S ribosomes, polyribosomes, by bound tRNA, and partially protected by the binding of polyU mRNA (Chapman & Noller, 1977; Moazed & Noller, 1986).

Several regions of 16*S* rRNA other than the 790 loop have also been implicated in subunit association (Meier et al., 1986; Meier et al., 1988; Agrawal & Burma, 1996). Agrawal and Burma demonstrated that an oligonucleotide probe hybridized to positions 811-820 of 16*S* rRNA in the 30*S* subunit significantly inhibited association with wild-type 50*S* subunits (Agrawal & Burma, 1996). Contrary to this result, it was previously shown that an oligonucleotide probe bound to nucleotide 815-823 of 16S rRNA had no effect on subunit association (Hill et al., 1988). Another study showed that 1416G mutated to 1416U greatly decreased association of mutant 30*S* subunits with wild-type 50*S* subunits and is proposed to be due to a structural change in the 30*S* subunit (Rottmann et al., 1988).

Interestingly, nucleotide 1416G has been shown to be reactive to chemical modification in 70*S* ribosomes but seems to be unreactive in free 30*S* subunits (Meier et al., 1986).

Firpo et al. (1996) provided evidence that when 1530G and 1531A in the 3' minor domain were mutated to 1530A and 1531G, subunits containing these mutations were deficient in the formation of 70*S* ribosomes. Lastly, mutations within the penultimate stem of 16S rRNA (1409-1491) which disrupted base-pairing resulted in severe subunit association defects (Firpo & Dahlberg, 1998).

The 2750 Loop

The 2750 loop is an 11 nucleotide single-stranded loop encompassing positions 2747-2757 in domain VI of 23S rRNA (Figure 2b). Very little information has been obtained regarding the role of this loop, 23S rRNA in general, or the 50*S* subunit in the process of subunit association. Hill et al. (1988) demonstrated that an oligonucleotide probe complementary to 23*S* rRNA bases 2750-2758 significantly inhibited subunit association. An oligonucleotide probe complementary to positions 2306-2313 partially inhibited subunit association indicating that this region may also be involved in subunit association (Hill et al., 1988). Chemical modification studies have shown that position 2751G of 23*S* rRNA is partially protected from modification in 70*S* ribosomes and that 2752C, 2757A and 2758A are weakly reactive in 50*S* subunits.

Base-Pairing Model

One proposal that suggests a molecular basis for subunit association involves rRNA-rRNA interactions between the 790 loop in 16*S* rRNA and the 2750 loop in 23*S* rRNA (Figure 4). Each of these single-stranded rRNA sequences is highly conserved , and more intriguingly, have the potential to form Watson-Crick base pairs with each other (Figure 4; Herr et al., 1979). This base-pairing model can be tested directly by making combinations of mutations in both the 790 and 2750 loops (Tapprich et al., 1989).

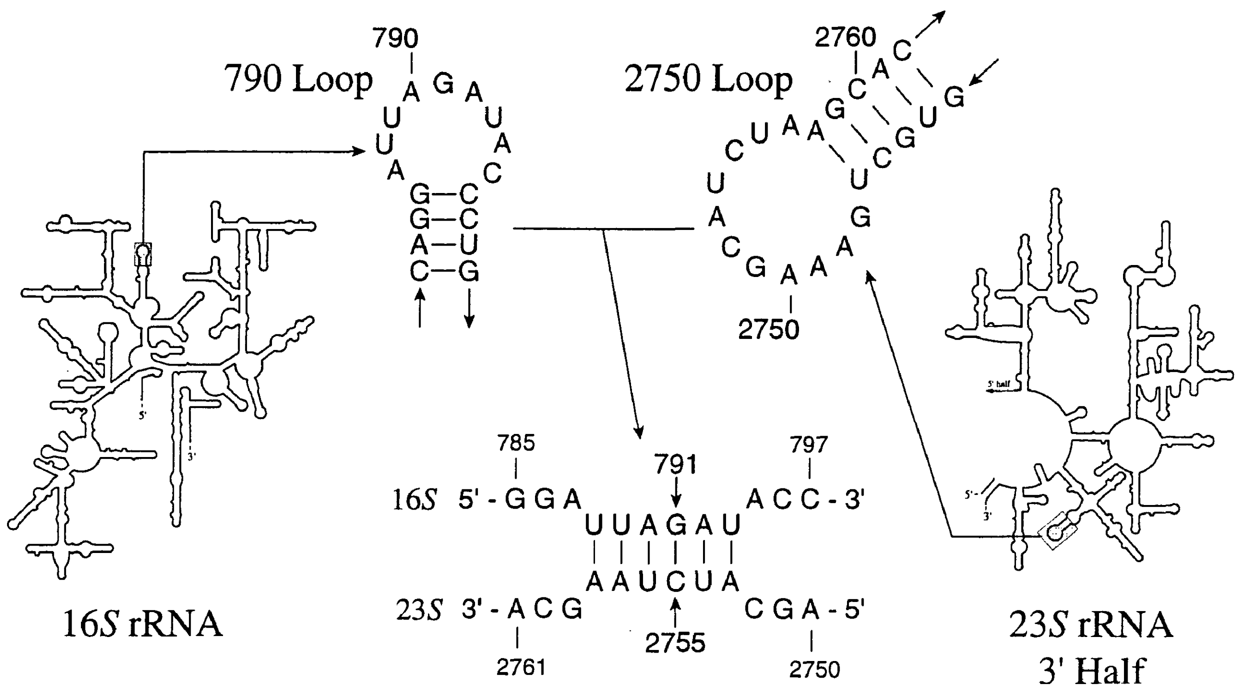

Figure 4. Proposed base-pairing model between the 790 loop of 16*S* rRNA and the 2750 loop of 23*S* rRNA in *E. coli* ribosomes. Indicated nucleotides, 791 of 16*S* rRNA and 2755 of 23*S* rRNA, were the focus of this study. Model originally proposed by Herr et al.(1979).

Model System to Study Mutant Ribosomes

The model system used in our laboratory to explore the structure and function of rRNA involves the study of site-directed mutations. The effects of ribosomes containing single nucleotide changes in rRNA on translation has been studied in *E. coli* DH-1 cells (Hanahan, 1983) expressing mutant rRNA from the pKK3535 rRNA expression vector (Figure 6; Brosius et al., 1981). In DH-1 cells, the pKK3535 expression vector is present in approximately 14 copies per cell and contributes approximately 50-70% of the rRNA in the cell (Jacob et al., 1987). Since the *E. coli* genome contains seven rRNA operons, there is always a background of wild-type ribosomes in the DH-1 cells that are expressing plasmid-borne mutant rRNA. As a result of this mixed population of ribosomes, results obtained from mutant strains are sometimes difficult to interpret.

Recently, our laboratory has obtained a strain of *E. coli*, a very generous gift from Dr. Cathy Squires (Tufts Univ.; Boston, MA), in which the seven rRNA operons have been deleted from the bacterial chromosome. This strain is known as the 7-deletion strain. The 7-deletion strain will undoubtedly result in new windows of opportunity for studies of rRNA structure and function. Since all seven chromosomal rRNA operons have been deleted, expression of rRNA for ribosomes is dependent upon a rRNA operon provided to the cell on a plasmid such as pKK3535. Thus the 7-deletion strain allows, for the first time, for a pure population of mutant ribosomes within cells expressing a plasmid encoding a rRNA mutation(s). With a pure population of mutant ribosomes, the interpretation of results will be less complex. This study has utilized both the DH-1 and 7-deletion strain systems to obtain a better understanding of the structure and function of rRNA.

Purpose of Study

The purpose of this study was to detail the role of the 790 loop of 16*S* rRNA and the 2750 loop of 23*S* rRNA in ribosomal subunit association. This was explored by creating all possible single mutations at position 2755C (A, G and U) within the 2750 loop using site-directed mutagenesis (Kunkel, 1985). All possible double mutations between position 791 within the 790 loop and 2755 were also constructed and analyzed. All single and double mutations were constructed in the pKK3535 expression vector, identified by PCR (Polymerase Chain Reaction) screening (see Materials and Methods) and confirmed by DNA sequence analysis (Sanger, 1977).

In vivo effects of rRNA mutants were studied by analyzing growth of DH-1 or 7-deletion strain cells containing mutant constructs. Effects of rRNA mutations were studied *in vitro* using ribosomal subunit association assays and chemical modification followed by primer extension to probe structure.

By characterizing the *in vivo* and *in vitro* effects of mutations at position 2755, this study provided one of the first investigations into the role of 23S rRNA in subunit association and translation. Recent models for ribosome activity have emphasized the critical role of the subunit-subunit interaction (Wilson & Noller, 1998b). By examining the 2755 mutations and the 791-2755 combination mutations, this study has provided some of the first direct mechanistic information about this interaction.

Chapter 2. Materials and Methods

Construction of rRNA Mutations

Site-Directed Mutagenesis

Site-directed mutagenesis was performed using an M13mp18 viral vector containing the SacI-BamHI fragment of the 23*S* rRNA gene (Figure 5). The SacI-BamHI fragment houses the 23*S* rRNA gene beginning at position 366 (*E. coli* numbering) and extending past the 3' end of the 23*S* rRNA coding sequence. Mutations were made at position 2755 (2755C) of 23*S* rRNA to 2755A, 2755G, and 2755U (Kunkel 1985). The 2755U mutation was previously constructed in the laboratory.

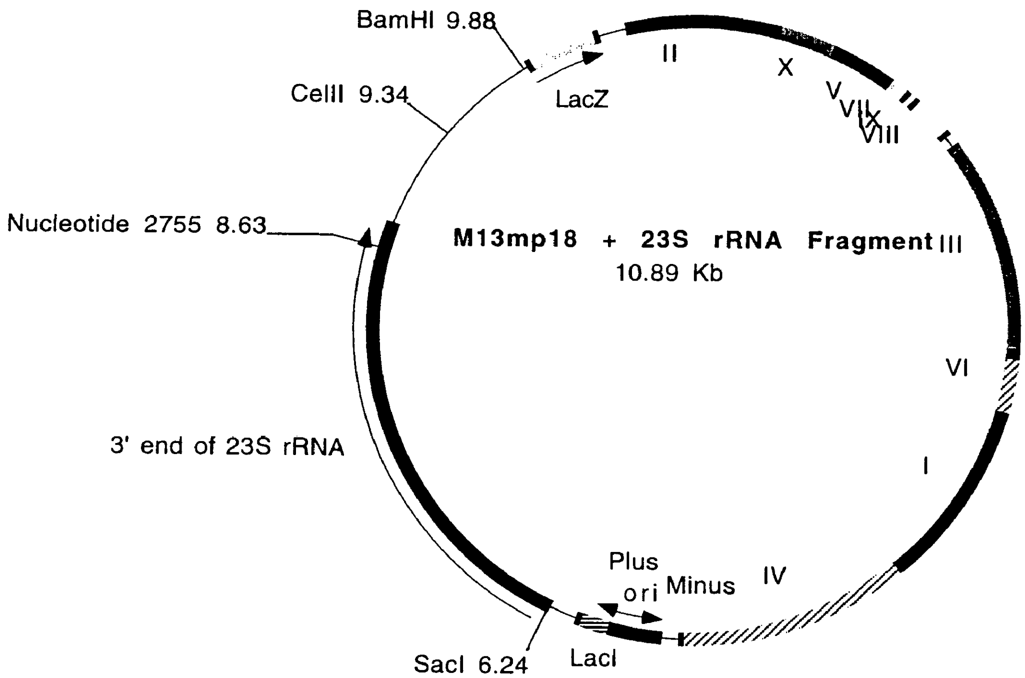

Figure 5. M13mp18 viral vector containing the SacI-BamHI fragment of the *rrnB* operon from *E. coli.* This viral vector was used to generate the single mutations at position 2755 of 23*S* rRNA.

Mutagenic Oligonucleotides

Two DNA oligonucleotides were designed to construct the mutations at position 2755, C2755A and C2755U. These two oligonucleotides, (Operon Technologies Inc.), were composed of the following sequences: 5'CGTGCTTATATGCTTT3' and 5'CGTGCTTACATGCTTT3'. Both oligonucleotides are complementary to *E. coli* 23*S* rDNA positions 2748-2763 with the exception of the mismatched nucleotide at position 2755. The oligonucleotides will anneal to the DNA template and upon replication the mismatched base at position 2755 allows for the incorporation of the complementary mutant nucleotide on the newly replicated strand.

The lyophilized oligonucleotides were resuspended in 200 µl of ddH2O and concentrations were determined spectrophotometrically by measuring absorbance at 260 nm and using an extinction coefficient of 33. Although the concentration of each oligonucleotide was different, 150 pmol/µl was a typical measured concentration. These samples were stored at -20°C.

Each oligonucleotide was phosphorylated on the 5' end using T4 polynucleotide kinase. In the phosphorylation reaction, 200 pmol of the oligonucleotide was placed in a total volume of 30 µl containing 100 mM Tris-HCl, pH 8.0, 10 mM $MgCl_2$, 5 mM DTT, and 0.4 mM ATP. To this mixture 4.5 units of T4 polynucleotide kinase (USB) was added and incubated at 37°C for 45 minutes. The reaction was stopped by heating at 65°C for 10 minutes and was then stored at -20°C.

Production and Isolation of Uracil-containing Phage DNA

The template strand for mutagenesis was M13mp18 (SacI-BamHI) single stranded DNA containing random incorporation of uracil (U-DNA). This template was generated by first adding 100 µL of M13mp18 phage stock which contained the SacI-BamHI fragment of 23*S* rDNA to 1.5 mL of 2XYT (per liter: 16 g tryptone, 10 g yeast extract, 10 g NaCl) containing 30 µg/mL chloramphenicol (CAM^{30}). Next, 100 µL of an overnight culture of

E. coli strain CJ236 was added and grown for six hours at 37°C at 200 oscillations/minute (opm). CJ236 cells are dut-, ung- which allows uracils to be randomly substituted for thymine in DNA synthesized within the cells. After the six hour growth, the cells were pelleted by centrifugation at 14,000 rpm in a microcentrifuge and the supernatant was isolated as a phage stock and stored at -20°C.

A 20 mL 2XYT- CAM^{30} culture containing 60 μl of an overnight culture of CJ236 was infected with 100 μl of the phage stock. This culture was grown for five hours at 37°C followed by chilling on ice for 10 minutes and pelleting the cells at 10,000 rpm for 15 minutes at 4°C in a Sorvall SS34 rotor. The supernatant was transferred to a fresh tube and the centrifugation step was repeated. The supernatant was transferred to another fresh tube and 100 μg of RNase A was added and incubated for 30 minutes at 37°C. One-third volume of 2.5 M NaCl-20% polyethylene glycol (PEG) was added and incubated overnight on ice at 4°C to precipitate the phage particles. The phage precipitate was pelleted for ten minutes at 10,000 rpm at 4.0°C in a Sorvall SS34 rotor. The supernatant was removed and the phage pellet resuspended in 250 μl of TE (10mM Tris-HCl, 1mM EDTA) followed by the addition of 2.0 μl of RNase A (10 mg/mL) and incubated for 30 minutes at room temperature.

This phage stock containing the single-stranded (ss) U-DNA was extracted two times with buffer saturated phenol (pH 7.9), two times with phenol/chloroform (25:24:1 phenol: chloroform: isoamyl alcohol) and two times with chloroform. The aqueous phase was separated and the ssU-DNA was precipitated using a standard ethanol precipitation protocol as follows. A volume of 3 M NaOAc equivalent to 0.1 volumes of the sample was added along with 2.5-3.0 volumes of 95% ethanol. This mixture was incubated at -20°C for 30 minutes. The precipitated ssDNA was pelleted at 14,000 rpm for 10 minutes in a microcentrifuge, washed with 100 μl of 70% ethanol and dried in a Savant Speed-Vac. The resultant dried phage ssDNA pellet was resuspended in 30μl ddH_2O and the concentration was determined by measuring absorbance at 260 nm using an extinction coefficient of 33.

Synthesis of the Mutagenic Strand

The mutagenic strand was synthesized by first annealing the phosphorylated mutagenic primer to the ssU-DNA template in a reaction containing 0.1 pmol ssU-DNA, 0.1, 1.0 or 10.0 pmol mutagenic oligonucleotide, 20 mM Tris-HCl, 2.0 mM MgCl2 and 50 mM NaCl in a total volume of 10μl. This reaction was placed in a 70°C water bath and allowed to cool at a rate of approximately 1.0°C/minute to 30°C over a 40 minute period followed by placement into an ice-water bath.

A 1:5 dilution of the Klenow Fragment of DNA polymerase (5 units/μl) was made using a cold solution of 100 mM potassium phosphate pH 7.0, 5.0 mM DTT and 50% glycerol to bring the concentration to 1 unit/μl. A 1:1 dilution of T4 DNA Ligase (10 units/μl) was made using a cold solution of 10 mM Tris-HCl pH 7.5, 50 mM KCl, 1 mM DTT and 50% glycerol to bring the concentration to 5 units/μl. With the reactions still in the ice-water bath the following components were added in the order listed: 1 μl of 10X synthesis buffer (5.2 mM dATP, dCTP, dGTP, & dTTP; 9.75 mM rATP; 227.5 mM Tris-HCl/pH 7.4; 48.75 mM $MgCl_2$; 279.5 mM DTT), 1 μl T4 DNA ligase (5 units) and 1 μl Klenow (1 unit) to make a total reaction volume of 13 μl.

These reactions were incubated on ice for 5 minutes, 25°C for 5 minutes and lastly at 37°C for 90 minutes. Following the 90 minute incubation, 90μl of TE was added and the reaction was stopped by freezing at -20°C.

Transformations and Identification of Mutations

E. coli XL-1 Blue competent cells were prepared as described by Hanahan (1989). This treatment allows the cells to take up plasmid DNA that is in solution with the cells. For each transformation, 200 μl of XL-1 Blue competent cells were placed in a cold 1.5 mL eppendorf tube on ice and 20 μl of the diluted synthesis reaction was added, mixed gently, and incubated on ice for 60 minutes. The cells were then placed at 42°C for 90 seconds and returned to ice. The transformed cells were added to 200 µl of log-phase XL-1 Blue cells and this mixture was then added to 3.0 mL of soft YT (per liter: 10 g tryptone, 5 g yeast extract, 10 g NaCl, 7.5 g agar) that had been cooled to 50°C. This mixture was mixed by vortexing and immediately poured on LB plates (per liter: 10 g tryptone, 5 g yeast extract, 10 g NaCl, 15 g agar). The soft YT was allowed to solidify and the plates were inverted and incubated overnight at 37°C.

Amplification of Phage ssDNA

Resultant viral plaques from the transformation of the mutagenesis extension-ligation mixes were cored from the LB plate and amplified to obtain the replicative form (RF) of the M13mp18 viral DNA. This was done by adding a cored plaque to 1.5 mL of 2XYT followed by the addition of 15 µl of an overnight culture of XL-1 Blue cells. This culture was incubated at 37°C at 200 opm for six hours. The cells were pelleted at 12,000 rpm in a 1.5 mL eppendorf tube in a microcentrifuge and were stored at -20°C.

A portion of the supernatant (750 µl) was saved as a phage stock and the remaining (750 µl) was added to 300 µl of 20% PEG/2.5 M NaCl and incubated on ice for 30 minutes. The phage particles were pelleted by centrifugation at 12,000 rpm for 10 minutes, the supernatant discarded, then the contents were centrifuged again to remove recalcitrant supernatant. The phage precipitate was resuspended in 180 µl of ddH_2O and 20 µl of 3M NaOAc was added. This solution was extracted once with phenol, twice with phenol/chloroform/isoamyl alcohol, and once with chloroform. To the resultant aqueous phase, 2.5 volumes of 95% ethanol was added and the remainder of the procedure was the same as described earlier for the standard ethanol precipitation.

Identification of Mutations Using Polymerase Chain Reaction (PCR)

A novel PCR-based screening technique was developed in collaboration with Dr. John Mullican to identify constructed mutations. This technique involves using pairs of DNA oligonucleotides that specifically amplify mutant ribosomal DNA (rDNA). Mutations were detected by using a common forward primer coupled with reverse primers containing unique 3' termini (A, C, G, or T). Only the primer with a 3' base complementary to the mutated base resulted in an extension, producing a fragment of known size. The technique was developed to provide reliable identification of mutant DNA molecules in several hours rather than the 3-4 days required for standard screening by DNA sequencing. In addition, multiple primer sets were used together in the same amplification reaction to facilitate the detection of combination mutant constructs. There are several points in the process of constructing mutations where this screening method was employed. Single-stranded phage DNA, phage RF DNA, and DNA cloned into an expression vector were all screened to identify the presence of mutations by using this method. Each of these options is described below. Lyophilized oligonucleotides were prepared as described previously.

Table 1. Oligonucleotides used in PCR screening reactions.

Oligonucleotide Name:	Oligonucleotide Sequence (5' → 3')	Complementary to rDNA nucleotides:	Size of rDNA fragment amplified (bp):
2755 forward	AGCTGGGTTTAGAACGTC	(23*S*) 2577-2594	195
2755 screen A	GGCAAGTTTCGTGCTTAT	(23*S*) 2772-2755	195
2755 screen C	GGCAAGTTTCGTGCTTAG	(23*S*) 2772-2755	195
2755 screen G	GGCAAGTTTCGTGCTTAC	(23*S*) 2772-2755	195
2755 screen T	GGCAAGTTTCGTGCTTAA	(23*S*) 2772-2755	195
791 forward	ATTGAGGCACGGTCGTCGG	(16*S*) 508-526	300
791 screen A	GTGGACTACCAGGGTATT	(16*S*) 808-791	300
791 screen C	GTGGACTACCAGGGTATG	(16*S*) 808-791	300
791 screen G	GTGGACTACCAGGGTATC	(16*S*) 808-791	300
791 screen T	GTGGACTACCAGGGTATA	(16*S*) 808-791	300

Screening Single-Stranded Phage DNA from a Viral Plaque

The earliest reliable point to screen for mutations is at the level of a viral plaque. To do this, a plaque was cored with a sterile pasteur pipet and placed in a 0.2 mL PCR tube with 50 μl of TE. The tube containing the plaque was heated at 95°C for five minutes. The heated plaque was vortexed for at least 10 seconds followed by centrifugation at maximum speed in a microcentrifuge for two minutes to pellet plaque debris. Next, 1-5 μl of the supernatant was removed to a new PCR tube as phage ssDNA template to screen in the PCR reaction. To this supernatant was added: 2 μl of 10X PCR buffer (500 mM KCl, 100 mM Tris-HCl, 15 mM, MgCl2, 0.01% gelatin), 2 μl of 10X dNTPs (2mM each of dATP, dCTP, dGTP and dTTP), 0.5 μl of the forward primer (0.083 μg/μl), 0.5 μl of the reverse primer with the unique 3' termini (0.083 μg/μl), 1.0 μl of Taq DNA polymerase (2.5 units), and ddH_2O to a final volume of 20 μl. This reaction was placed in a thermalcycler and programmed to run the following cycles:

95°C, 5 min. → (60°C, 5 sec.→72°C, 30 sec.→94°C, 5 sec.) X 25 cycles → 60°C, 1.0 min. → 72°C, 1.0 min. → 4.0°C, hold.

(Note: For each primer set, the annealing temperature may require adjustment for optimization of different reactions)

After completion of these cycles, 5 μl of the reaction was removed and analyzed on an agarose gel. If the mutation was present in the phage plaque, the reverse primer with the 3' deoxynucleotide complementary to the mutation extended along with the common forward primer resulting in a PCR product of known length which was detected on the agarose gel.

Screening Phage RF DNA from Cells Infected with Virus

RF DNA from cells isolated from the amplification of virus was also screened for the presence of mutations. Following phage amplification, the cell pellet was saved and phage RF DNA was isolated from these cells according to the protocol from the Promega Wizard™ Miniprep DNA purification system. From this isolated RF DNA, 10 ng or no more than 1/10 volume of the eluant was used in the screening reaction as described above in Screening Single-Stranded Phage DNA from a Viral Plaque.

Screening Plasmid DNA from a Bacterial Colony

Mutations carried on the plasmid pKK3535 were screened directly from a bacterial colony. This was accomplished by first using a sterile toothpick and suspending a bacterial colony in 50 μl ddH_2O by vortexing the tip of the toothpick in an eppendorf tube. This toothpick was then used to streak the bacteria on solid media at the appropriate temperature for later recovery. The colony suspension was then heated to 95°C (or boiled) for 5 min. to lyse the cells and allowed to cool to room temperature. The lysate was vortexed for several seconds followed by pelleting cell debris by centrifugation at maximum speed in a microcentrifuge for 2 minutes. The supernatant contained the plasmid DNA and was used in the PCR screening reaction as described above in Screening Single-Stranded Phage DNA from a Viral Plaque.

Cloning Mutations into the pKK3535 Expression Vector

The pKK3535 Expression Vector

The pKK3535 expression vector is an 11,864 base pair (bp) plasmid containing the *E. coli rrnB* operon with the natural promoters, P1 and P2, and terminators, T1 and T2, a colE1 origin of replication and an ampicillin resistance gene (Figure 6; Brosius et al., 1981). This is a low copy plasmid and is present in approximately 14 copies per cell in *E.*

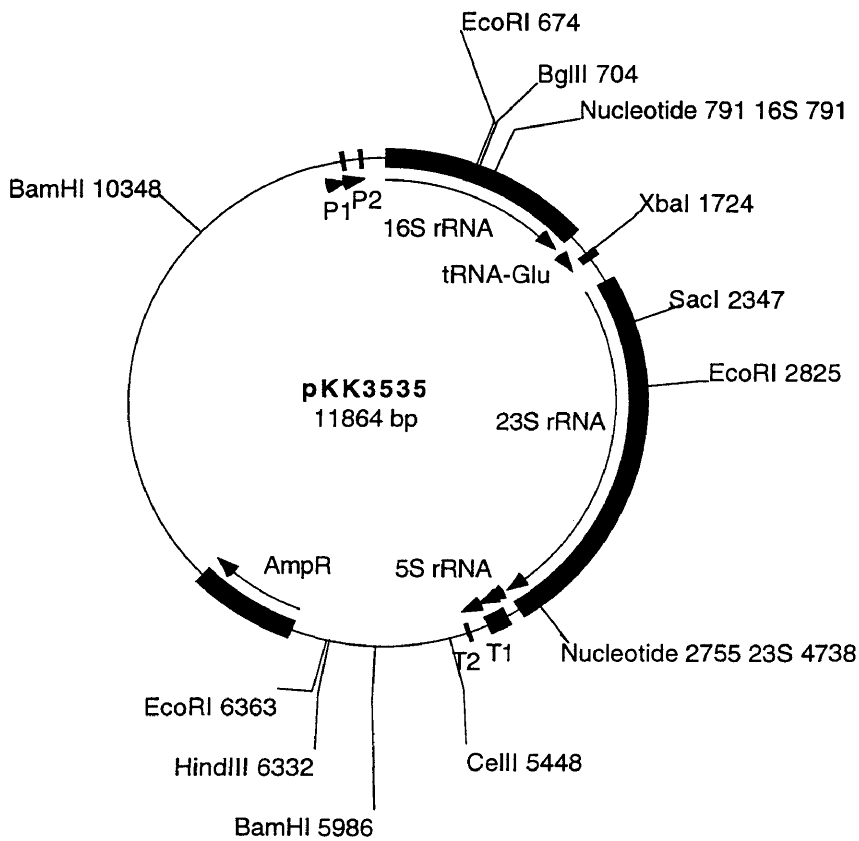

Figure 6. Map of the pKK3535 expression vector. This expression vector contains the *E. coli rrnB* operon with the natural promoters (P1 and P2) and terminators (T1 and T2), and an ampicillin resistance gene (Brosius et al., 1981).

coli DH-1, contributing to the production of 50-70% of the rRNA in DH-1 cells (Jacob et al., 1987).

Large Scale Plasmid and RF Preparations

To facilitate the cloning of mutated rDNA into the expression vector pKK3535, large scale DNA preparations were accomplished. M13mp18 RF DNA containing the mutation and wild-type pKK3535 were prepared separately. The large scale RF preparation involved placing 2.5 mL of an overnight culture of XL-1 Blue cells into a sterile 13 mm x 100 mm test tube. This culture was inoculated with 0.5 mL phage stock from a mutant phage isolate and let stand at room temperature for 5 minutes. The infected culture was then added to 250 mL of 2XYT prewarmed to 37°C in a fernbach flask and incubated at 37°C at 170 opm for six hours. Harvesting of the infected cells and isolation of RF DNA was done according to Maniatis et al (1989).

The large scale pKK3535 plasmid preparation required inoculating 10 mL of LB (per liter: 10 g tryptone, 5 g yeast extract, 10 g NaCl) containing 0.2 mg/mL ampicillin (LB-amp^{200}) with a colony containing the plasmid and growing overnight at 37°C. The next morning another 10 mL culture was inoculated with 100 µl of the overnight culture and grown at 37°C until the culture reached an OD_{600} of 0.4-0.6 (4-6 hrs.). One liter of LB- amp^{200} in a fernbach flask was then inoculated with 5 mL of the log phase culture and the culture was grown overnight at 37°C. Harvesting of the cells and isolation of DNA was accomplished according to Maniatis et al. (1989).

Restriction Endonuclease Digests

Single Mutants

To obtain the proper DNA fragments for cloning, the pKK3535 plasmid and the M13 RF DNA were digested with the SacI and CelII restriction endonucleases. Digestion with these enzymes yields a 8,763 bp pKK3535 vector fragment and a 3,101 bp insert fragment carrying the mutation from the M13mp18 RF DNA. The plasmid and RF CelII digests each required incubating 40 μg of DNA in a 150 μl reaction containing a 10% volume of Amersham 10X buffer H (500 mM Tris-HCl pH 7.5, 100 mM $MgCl_2$, 10 mM DTT, 1 M NaCl) and 40 units CelII (Amersham). This reaction was incubated at 37°C overnight and was stopped by a standard phenol extraction/ethanol precipitation procedure as described earlier. The resultant CelII digested DNA was resuspended in 40 μl ddH_2O. The SacI digest was completed on this DNA by combining the sample with 0.1 volumes of Amersham 10X buffer L (100 mM Tris-HCl pH7.5, 100 mM $MgCl_2$, 10 mM DTT) and 48 units of SacI (Amersham). This reaction was also incubated at 37°C overnight and was stopped by a standard phenol extraction/ethanol precipitation procedure.

The CelII-SacI digested DNAs were separated by size using agarose gel (1%) electrophoresis. The 8,763 bp pKK3535 vector fragment and the 3,101 bp M13mp18 insert fragment were eluted from the gel according to the Qiagen QIAquick Gel Extraction Kit in 30 μl ddH_2O. Ten percent of each sample was assayed on a 1% agarose gel. To make pKK3535 constructs containing mutations at position 2755, 10 ng of vector and 20 ng of insert (a 1:5 vector : insert molar ratio) were incubated for 24 hrs at 16°C in a 20 μl ligation reaction consisting of 66mM Tris-HCl/pH 7.6, 6.6 mM $MgCl_2$, 10 mM DTT, 66 μM ATP and 10 units T4 DNA ligase (Amersham).

Following the ligation reactions, 5 μl of each reaction was diluted 1:1 with ddH_2O and transformed into competent *E. coli* DH-1 and MDA6646 cells (Hanahan, 1989) as follows. The two different cell types are needed because of maintenance of different copy numbers of the pKK3535 constructs within the cells. MDA6646 cells maintain a lower copy number of pKK3535 constructs and thus these cells are more tolerant of deleterious mutations expressed from the plasmid. Competent cells (200 μl) were thawed on ice 5-10 minutes. The cells were mixed gently and 10 μl of the diluted ligation reactions were added and incubated on ice for 60 minutes. The cells were then heat shocked at 42°C for 90 seconds followed by quenching on ice for at least 2 minutes. Next, 0.9 mL of LB was added to the cells, mixed and incubated at 37°C for 45 minutes. The transformed cells were pelleted by centrifugation in a microcentrifuge at maximum speed, the supernatant was removed and the cells were resuspended in 150 μl of LB. Lastly, the cells were plated on LB-amp^{200} plates and incubated overnight at 37°C.

Transformants were screened for the presence of mutations using the colony-boil PCR screening technique described earlier. A colony that screened positive for the desired mutation was confirmed by DNA sequence analysis (Figure 7a-7d). Sequencing reactions were performed according to the protocol of Stratagene for the Cyclist™ Exo$^-$ Pfu DNA sequencing kit.

Double Mutants

All possible combinations of double mutants at position 791 of 16*S* rRNA and 2755 of 23*S* rRNA were also constructed in the pKK3535 expression vector (see Table 2). The 791 mutations were previously constructed in pKK3535 in the laboratory. The double mutant constructs were made by a simple "cassette exchange" of the 1020 BglII-XbaI restriction fragment of pKK3535. This fragment contains the 16*S* rRNA gene beginning at position 704 and extending 182 nucleotides past the 3' end of the 16*S* rRNA coding sequence (Figure 6).

Table 2. Mutations Constructed in the pKK3535 Expression Vector

pKK2755A
pKK2755G
pKK2755U
pKK791A-2755A
pKK791A-2755G
pKK791A-2755U
pKK791C-2755A
pKK791C-2755G
pKK791C-2755U
pKK791U-2755A
pKK791U-2755G
pKK791U-2755U

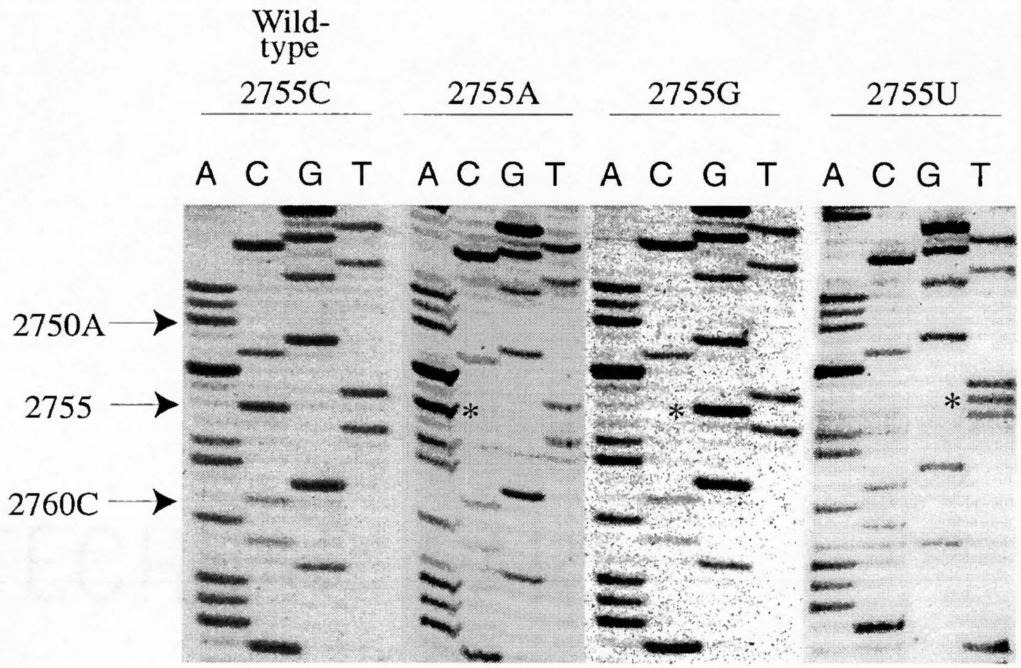

Figure 7a. DNA sequence analysis of single mutations at position 2755 of *E. coli* 23*S* rRNA. Each mutation is indicated with an asterisk.

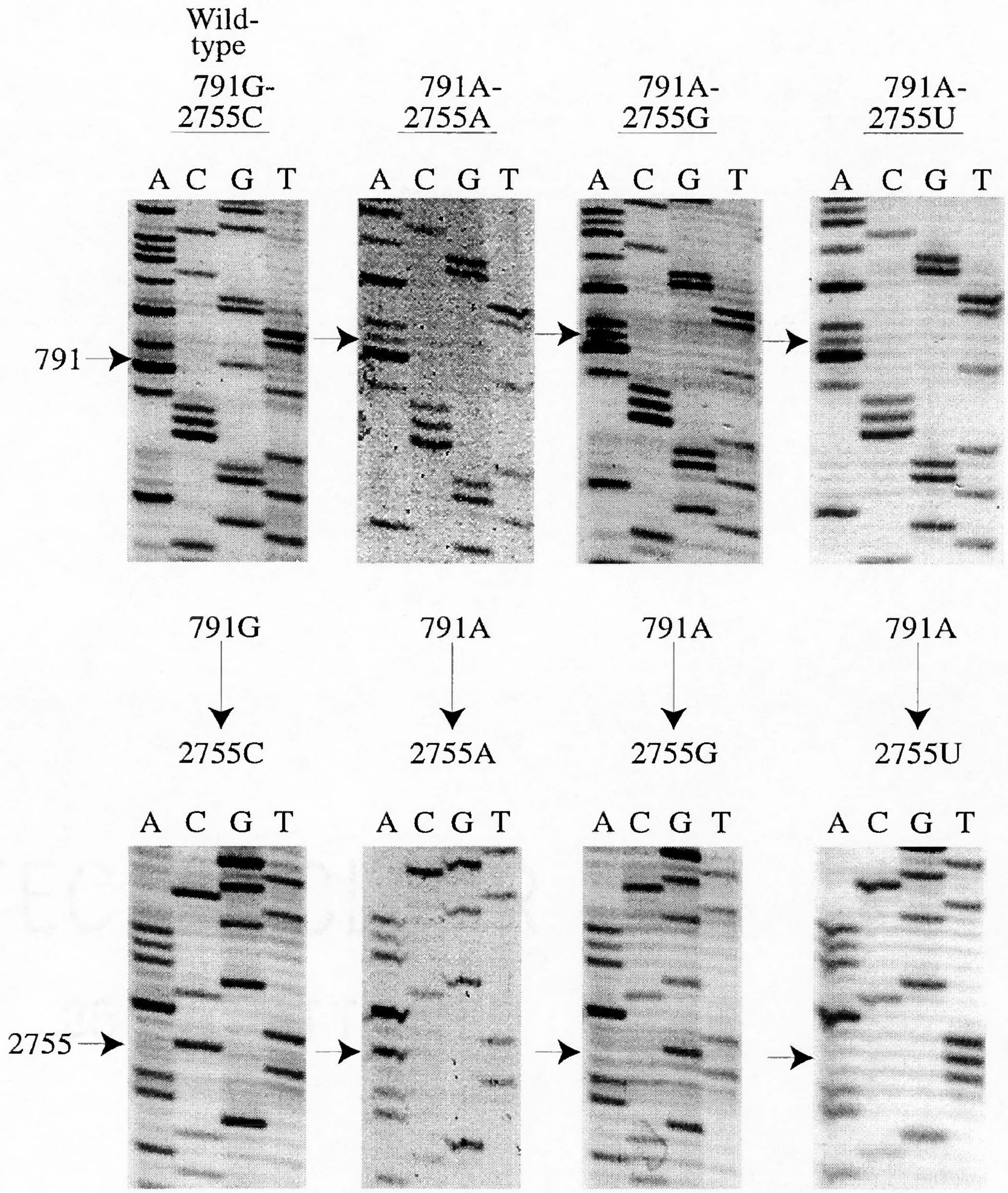

Figure 7b. DNA sequence analysis of double mutations at positions 791 of 16*S* rRNA and 2755 of 23*S* rRNA in *E. coli*. Each mutation is indicated with an arrow.

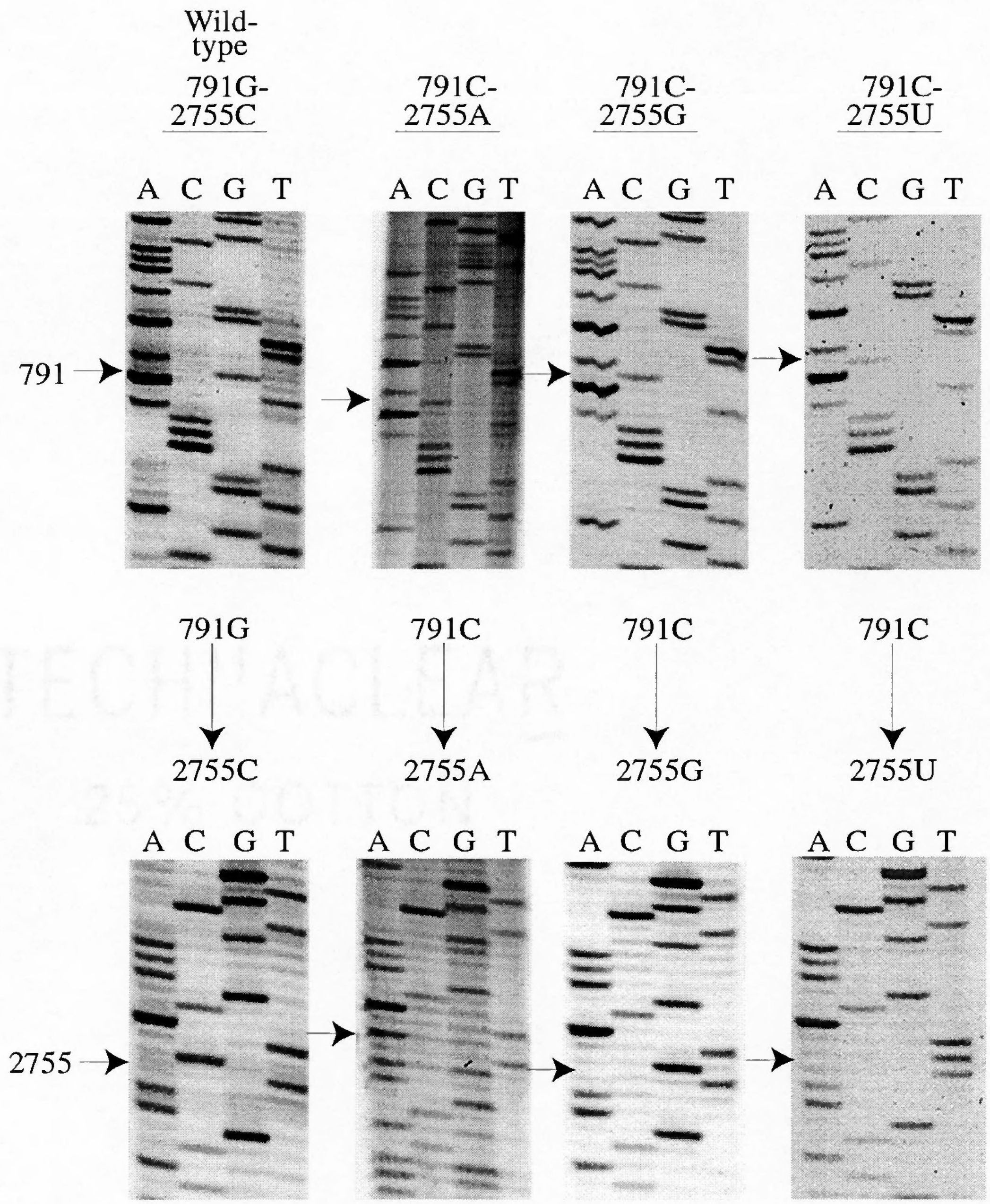

Figure 7c. DNA sequence analysis of double mutations at positions 791 of 16*S* rRNA and 2755 of 23*S* rRNA in *E. coli*. Each mutation is indicated with an arrow.

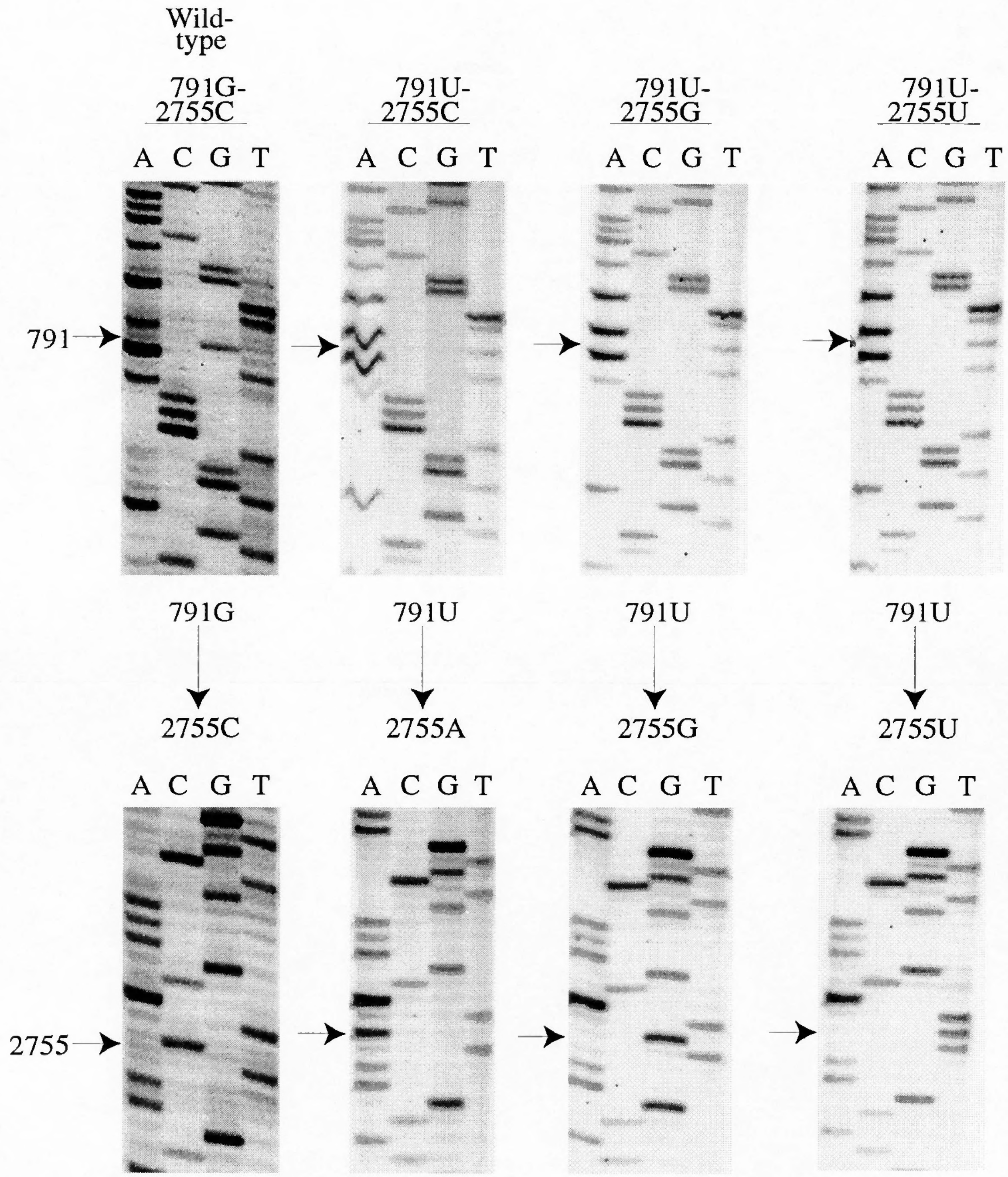

Figure 7d. DNA sequence analysis of double mutations at positions 791 of 16*S* rRNA and 2755 of 23*S* rRNA in *E. coli*. Each mutation is indicated with an arrow.

Large scale DNA preparations of all single mutants at position 791 (pKK791A, C, and U) as well as 2755 (pKK2755A, G, and U) were completed as described earlier. Each DNA preparation was digested with BglII and XbaI endonucleases. Each digest consisted of 20 μg DNA, 20 μl 10X universal buffer (1M KOAc, 250 mM Tris-Acetate pH 7.6, 100 mM MgOAc, 5 mM ß-mercaptoethanol, 100 μg/ml BSA), 2 μl BglII (24 units), 2 μl XbaI (20 units), and water to a final volume of 200 μl. These reactions were incubated at 37°C overnight, phenol extracted, ethanol precipitated and resuspended in 20 μl ddH_2O.

The BglII-XbaI digested DNA fragments were separated on an agarose gel and eluted as described previously. For the pKK2755 mutant constructs, the 10,844 bp fragments containing the mutations at position 2755 were eluted and used as vector in the ligation reactions. The 1,020 bp fragments from the pKK791 mutant constructs were eluted and used as insert in the ligation reactions. Ligation reactions, transformations, identification and confirmation of mutations were performed as described for the single mutation constructs. Upon confirmation of all single and combination mutation constructs, each construct was transformed into competent 7-deletion strain cells as described previously.

Isolation of Ribosomes and Ribosomal Subunits

Ribosomes and ribosomal subunits were isolated following the procedure of Tapprich et al. (1989) and is briefly outlined below. Cells containing the plasmid of interest were grown in 1 liter of LB or LB-amp^{200} (if antibiotic pressure was not needed for cells to retain the plasmid, cells were grown in the absence of antibiotic) to OD_{600}=0.4-0.6. Cells were chilled on ice for 10 min and harvested by centrifugation at 5,000 rpm for 10 min in a Sorvall GS3 rotor. The pelleted cells were resuspended in 15 mL of buffer A (25 mM Tris-HCl pH 7.6, 10 mM $MgCl_2$, 150 mM KCl, 1 mM DTT) and pelleted again for 10 min at 4°C at 5,000 rpm this time in a Sorvall SS34 rotor. The buffer was discarded and the cell pellet was stored at -70°C. Cells were thawed on ice and broken open with 2.5X the cell mass of alumina by grinding with a mortar and pestle on ice. When finished grinding, 200 units of RNase-free DNase I (Worthington Biochemicals) was added, mixed well and incubated on ice for 5 min. The ground cell paste was transferred to a prechilled SS34 tube using 20 mL of buffer A and centrifuged at 12,000 rpm for 10 min at 4°C to remove alumina. The supernatant was transferred to a fresh SS34 tube and was centrifuged at 16,000 rpm for 60 min to remove cellular debris. The supernatant was decanted into a 30 mL Oakridge tube and was centrifuged for 3 hrs at 60,000 rpm in a Beckman 70 Ti rotor to pellet ribosomes. Resulting ribosome pellets were rinsed with 10 mL buffer B (10 mM Tris-HCl pH 7.6, 15 mM $MgCl_2$, 500 mM NH_4Cl, 1 mM DTT) and resuspended in 10 mL buffer B overnight on a tilt-table at 4°C. This ribosome suspension was transferred to an SS34 tube and centrifuged again at 16,000 rpm for 60 min at 4°C. The supernatant was gently layered onto a 10 mL sucrose cushion composed of 5 mL of 30% sucrose and 5 mL of 10% sucrose each made with buffer B and centrifuged 18 hrs at 45,000 rpm at 4°C. The resultant ribosome pellet was rinsed with 5 mL TC-70 buffer (25 mM Tris-HCl pH 7.6, 60 mM KCl, 10 mM $MgCl_2$, 1 mM DTT) followed by resuspension in 0.5 mL of the same buffer overnight at 4°C on a tilt-table. Ribosome concentrations (mg/mL) were determined by measuring absorbance at 260 nm using an extinction coefficient of 14.5. The concentration in mg/mL was then divided by the molecular weight of 70*S* ribosomes (2.7×10^6 g/mol) to yield the concentration in pmol/mL. An average concentration of ribosomes purified from a one liter culture of cells was approximately 30 pmol/µl (81 µg/µl). Ribosomes purified by this method were further fractionated for the *in vitro* assays discussed later.

In Vivo Assays

Bacterial Doubling Times

Doubling times of *E. coli* 7-deletion strain cells containing the wild-type pKK3535 plasmid as well as cells containing mutant plasmids were determined using a Klett-Sommerson colorimeter. Cultures containing 25 mL of LB in a sidearm flask were incubated with cells from a spread plate suspended in 1 mL of LB. The Klett readings of this culture at time 0 were between 8 and 12. Flasks were incubated in a New Brunswick shaking water bath at 37°C with shaking at a vigorous setting of 7. The turbidity of the cultures was measured every 20 min for wild-type constructs and constructs in which cell growth was not greatly slowed; very slow growing constructs were measured every 30 min. The Klett readings from the logarithmic portion of the growth curve were used to determine doubling times.

In Vitro Assays

Ribosomal Subunit Reassociation Assays

Ribosomes purified from cells according to the methods described above exist primarily as 70*S* (associated) couples. To dissociate the subunits completely, these ribosomes were dialyzed against a buffer containing 1.5 mM $MgCl_2$, 25 mM Tris-HCl pH 7.6, 150 mM KCl and 1 mM DTT.

One milliliter of ribosomes diluted to a concentration of 5 mg/ml was placed in dialysis tubing (3 mm diameter, molecular weight cut-off of 10,000 Da) and dialyzed overnight at 4°C in 30-50 buffer (25 mM Tris-HCl pH 7.6, 150 mM KCl, 1.5 mM $MgCl_2$, 1 mM DTT) to completely separate ribosomes into 30*S* and 50*S* subunits. Following dialysis, the concentration of the dissociated ribosomal subunits was determined as previously described.

To ensure the complete dissociation of ribosomal subunits following dialysis, 250 μg of the dissociated ribososmes were loaded onto a 5-30% sucrose gradient made with 30-50 buffer and centrifuged in a Beckman SW-41 rotor at 4°C for 4.5 hrs at 35,000 rpm. The dissociated subunits were separated by density in the gradient, which was then pumped through an Isco Apparatus UA-5 Absorbance/Fluorescence Detector at a pump speed of 3 mL/min. The absorbance of the ribosomal fractions was measured at 260 nm and profiles were generated on chart paper with a chart speed of 60 cm/hr by the Isco detector. These profiles verified that the ribosomes were completely dissociated into 30*S* and 50*S* subunits.

Once complete dissociation of subunits was confirmed, 250 μg of equimolar quantities of 30*S* and 50*S* ribosomal subunits were reassociated using increasing concentrations of $MgCl_2$. Since Mg^{2+} promotes subunit association, the formation of 70*S* ribosomes is very sensitive to the $MgCl_2$ concentration. The dialyzed subunits (250 μg) were incubated at 37°C for one hour in a 250 μl volume consisting of 6 or 10 mM $MgCl_2$, 25 mM Tris-HCl pH 7.6, 60 mM KCl and 1 mM DTT. Following the incubation, these samples were loaded onto a 5-30% sucrose gradient made with the same buffer as that contained in the incubation step. The gradients were centrifuged and pumped through the Isco detector as described previously. These gradients demonstrated the association affinity between wild-type 30*S* subunits and mutant 50*S* subunits, or mutant 30*S* subunits and mutant 50*S* subunits.

Primer Extensions

Primer extension reactions were done on rRNA extracted from ribosome preparations to determine the amount of mutant rRNA in the ribosomal pools (Sigmund et al., 1988). rRNA was isolated by extracting ribosomes three times with phenol and twice with chloroform followed by standard ethanol precipitation as described previously. Lyophilized oligonucleotides were obtained from Operon for use in the primer extension reactions and were prepared as described previously. However, these oligonucleotides were gel purified using polyacrylamide gel electrophoresis (PAGE). Each oligonucleotide was purified by running 50 μg on a 20% polyacrylamide gel (8 M urea, 90 mM Tris-HCl, 90 mM boric acid, 2 mM EDTA pH 8.0, 20% acrylamide-bisacrylamide 19:1) for two hours at 400 volts. The oligonucleotide bands were visualized by UV shadowing on a thin layer chromatography plate and were cut out using sterile razor blades. The gel slices containing the primers were placed in an eppendorf tube with 200 μl of TE and incubated at 37°C overnight. The buffer was removed to a new eppendorf tube and polyacrylamide particles were removed by centrifugation at maximum speed for 2 minutes in a microcentrifuge. The buffer was again removed to a fresh eppendorf tube and oligonucleotides were precipitated by standard ethanol precipitation, resuspended in 50 μl TE and concentrations determined at described previously.

The 2755 primer extension oligonucleotide has the sequence 5'CTCGGGGCAAG TTTCGTG3' and is complementary to 23*S* rRNA bases 2759-2777. When used with ddG, the primer extension reaction for position 2755 will yield a 4 base extension for wild-type rRNA and a 7 base extension for mutant rRNA. The 791 primer extension oligonucleotide has the sequence 5'CGGCGTGGACTACCAGGG3' and is complementary to 16*S* rRNA bases 795-812. When used with ddC, the primer extension reaction for position 791 will yield a 4 base extension for wild-type rRNA and a 9 base extension for mutant rRNA.

Primer extension oligonucleotides were 5' end-labeled by incubating 10 pmol of gel purified primer with 50 μCi [δ-^{32}P]dATP in a 20 μl reaction containing 50 mM Tris-HCl pH 7.6, 10 mM $MgCl_2$, 10 mM ß-mercaptoethanol, and 10 units T4 polynucleotide kinase. The reaction was incubated at 37°C for 45 min followed by 70°C for 10 min to heat-kill the kinase. The ^{32}P-labeled oligonucleotides were annealed to the rRNA templates in a 10 μl reaction consisting of 1 pmol of labeled primer, 2 pmol of rRNA, 50 mM Tris-HCl pH

8.3, 60 mM NaCl, 10 mM DTT and 6 mM MgOAc. Annealing reactions were heated to 75°C and slow-cooled to approximately 30°C. Five microliters of annealed oligo-RNA complexes were extended in 10 μL reaction volumes with 0.5 μl of AMV reverse transcriptase (RT, 7.5 units) and 4.5 μl of ddNTP mix (50 mM Tris-HCl pH 8.3, 60 mM NaCl, 20 mM DTT, 6 mM MgOAc, 0.25 mM of three dNTPs and one ddNTP). For example, to detect the G791A mutation, the dNTPs in the mix were dATP, dCTP and dGTP while the ddNTP was ddTTP. The extension reactions were incubated at 45°C for 20 min and stopped with 4 μl of stop solution (0.1% bromophenol blue, 0.1% xylene cyanol, 10 mM EDTA, 90% deionized formamide). The reactions were placed in a boiling water bath for 2 min and 4 μl of each reaction was run on a 12% polyacrylamide gel at 65 Watts for 1 hr 40 min. The resultant gels were dried and exposed to X-ray film in a film cassette for 3-8 hrs depending on the intensity of the radioactive signal.

Structure Probing

Structure probing with dimethylsulfate (DMS) was done on 70*S* ribosomes and 30*S* ribosomal subunits ("ribosomes" will refer to 70*S* ribosomes or 30*S* subunits in this section) to monitor the structure of the rRNA in and around the 790 loop in 16*S* rRNA and the 2750 loop in 23*S* rRNA. DMS modification reactions were set up in 100 μl volumes containing 50 pmol of ribosomes, 80 mM K-Cacodylate pH 7.2, 20 mM $MgCl_2$, 100 mM NH_4Cl and 1.5 mM DTT. The ribosomes were heat activated at 42°C for 20 min followed by incubating on ice for 10 min. The DMS modification solution contained 2 μl of a 1:5 dilution of 100% DMS in 95% ethanol. This solution was added to each reaction and gently mixed with a pipettman. For each reaction in which ribosomes were modified, an unmodified reaction was also performed. Ribosomes were carried through the experiment in exactly the same conditions as the modified samples with the exception of the addition of DMS. Reactions were incubated at 37°C for 10 min and were stopped by adding 25 μl of DMS stop buffer (1 M Tris-HCl pH 7.5, 1 M ß-mercaptoethanol and 0.1 M EDTA). To precipitate the modified ribosomes, 300 μl of 95% ethanol was added and the reactions were placed at -20°C for at least 30 min. Modified ribosomes were pelleted by centrifugation at maximum speed for 10 min in a microcentrifuge. The ribosome pellet was washed with 100 μl of 70% ethanol and then dried in a Savant Speed-Vac. Dried ribosome pellets were redissolved in 200 μl of 0.3 M NaOAc pH7.0, 0.5% SDS and 5 mM EDTA. The resuspended ribosomes were extracted three times with phenol and two times with chloroform and the recovered rRNA was precipitated two times with 95% ethanol. Precipitated rRNAs were dried in a Savant Speed-Vac and were resuspended in TE pH 8.0 to a final concentration of 1 μg/μl.

Two oligonucleotides were used for extension reactions on modified rRNAs. The oligonucleotide used for the extension reactions on the modified rRNA for the 790 loop has the sequence 5'GACTTAACGCGTTAGCT3' and is complementary to 16S rRNA nucleotides 860-876. The oligonucleotide used for the extension reactions on the modified rRNA for the 2750 loop has the sequence 5'CCTTCAGGACCCTTAAAG3' and is complementary to 23S rRNA nucleotides 2805-2812.

Oligonucleotides were 5' end-labeled with [δ-^{32}P]dATP as described previously for primer extensions. Labeled oligonucleotides were annealed to the modified rRNA templates in 10 μl reactions containing 2 μg of rRNA, 2 pmol of labeled primer, 50 mM Tris-HCl pH 8.3 and 40 mM KCl. These reactions were heated to 75°C and slow-cooled to 30°C. To the annealing reactions, 5 units of AMV reverse transcriptase in 2 μl of 50 mM Tris HCl pH 8.3, 40 mM KCl and 6 mM $MgCl_2$ was added and mixed. Aliquots containing 2 μl of the annealing-RT mixes were added to 2 μl of A, C, G and T termination mixes (50 mM Tris-HCl pH 8.3, 40 mM KCl, 6 mM $MgCl_2$, 1 mM each dNTP and 0.1 mM of one ddNTP) for rRNA sequencing or to 2 μl of extension mix (100 mM Tris-HCl pH 8.3, 80 mM KCl, 12 mM $MgCl_2$ and 4 mM of each dNTP) for extension on unmodified or modified rRNAs. These reactions were then incubated at 45°C for 20 min and stopped by the addition of 2 μl of stop solution. Reactions were heated to at least 90°C for five min and were quenched on ice followed by loading 2.5 μl of each reaction onto a 12% polyacrylamide gel. Gels were run at 65 Watts for 2.5 hrs (probing 2750 loop) or 4.0 hrs (probing 790 loop). The resultant gels were dried and exposed to X-ray film in a film cassette at room temperature.

Chapter 3. Results

Construction of rRNA Mutants

Position 2755C of 23*S* rRNA was mutated to 2755A and 2755G using *in vitro* site-directed mutagenesis on M13mp18 ssU-DNA as outlined by Kunkel (1985). M13mp18 RF DNA containing each mutation was identified by PCR screening (Figure 8). Figure 8 shows an example of screening wild-type, two mutants at position 2755, and a double mutant between positions 791 and 2755 resolved on a 1% agarose gel. The single mutations at position 2755 generated a PCR fragment of 195 bp and are indicated with an asterisk. The double mutant construct shows a 195 bp band generated for the mutation at position 2755 and a 300 bp band generated for the mutation at position 791 (these bands are also indicated by an asterisk). The screening reactions contain both plasmid and chromosomal DNA, so a band also appears in the lane corresponding to the wild-type sequence due to the presence of the seven wild-type rRNA operons on the chromosome (these bands are indicated by arrows). Thus, positive mutant screens revealed both a wild-type band and the mutant band.

The SacI-CelII restriction fragments containing the C2755A and C2755G mutations were cloned into the expression vector pKK3535 to produce pKK2755A and pKK2755G. These constructs were transformed into competent *E. coli* cells (MDA6646, DH-1 or 7-deletion strain) and cells transformed with the mutant plasmid were identified using the

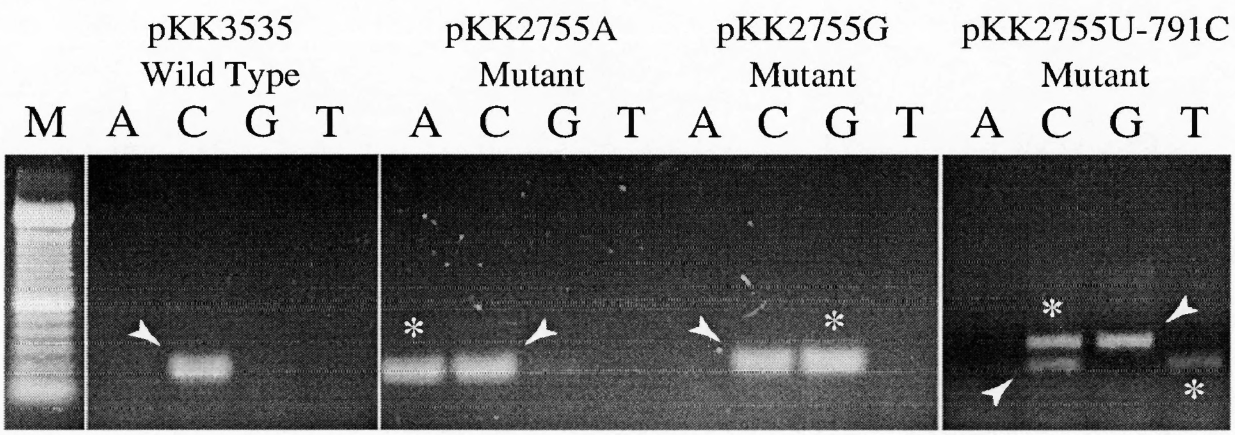

Figure 8. PCR-based screen of pKK3535 mutant constructs. Lanes A, C, G and T correspond to primers designed to detect pKK2755 or pKK791 A, C, G and T mutants respectively. The pKK2755 and pKK791 PCR primers amplify 195 bp and 300 bp DNA fragments respectively. Amplification of genomic (wild-type) background ribosomal DNA is present in all reactions and are indicated by arrowheads. PCR products from mutant templates are indicated by asterisks. 100 bp ladder (BRL) was used as the molecular weight standard (M).

PCR screening method. Strains that screened positive for the presence of the mutant plasmid were confirmed by DNA sequence analysis (Figure 7a).

Upon completion of the single-mutation cloning procedures, the 791-2755 double-mutant constructs were generated. The 1020 bp BglII-XbaI restriction fragments containing the mutations at position 791 were successfully isolated from large scale plasmid preparations of the 791 single mutants in pKK3535 and were cloned into the 10,844 bp pKK3535 vector fragments carrying the mutations at position 2755. Thus each possible combination of double mutations between positions 791 of 16*S* rRNA and 2755 of 23*S* rRNA were created. These double mutant constructs were successfully transformed into competent *E. coli* cells (MDA, DH-1 or 7-deletion strain), identifed by PCR screening and confirmed by DNA sequencing (Figures 7b-7d, 8).

Effects of rRNA Mutations *In Vivo*

Growth in MDA6646 and DH-1

All single and combination mutant constructs were transformed into MDA6646 cells and colony morphologies were monitored on LB-amp^{200} solid media at 37°C. All mutant constructs were viable in MDA6646 and displayed no differences in growth phenotype on solid media (data not shown).

The growth of *E. coli* strain DH-1 cells containing the pKK2755A, G and U constructs were monitored by observing colony morphology on LB-amp^{200} solid media at 37°C. These constructs demonstrated the same growth phenotype on solid media as cells containing wild-type pKK3535 with the exception of the 2755U single mutant which grew slightly slower (Figure 9).

E. coli DH-1 cells were also transformed with the double mutant constructs and colony morphology was observed on LB-amp^{200} solid media at 37°C. The following double mutant constructs were unable to support cell growth when transformed into E. coli

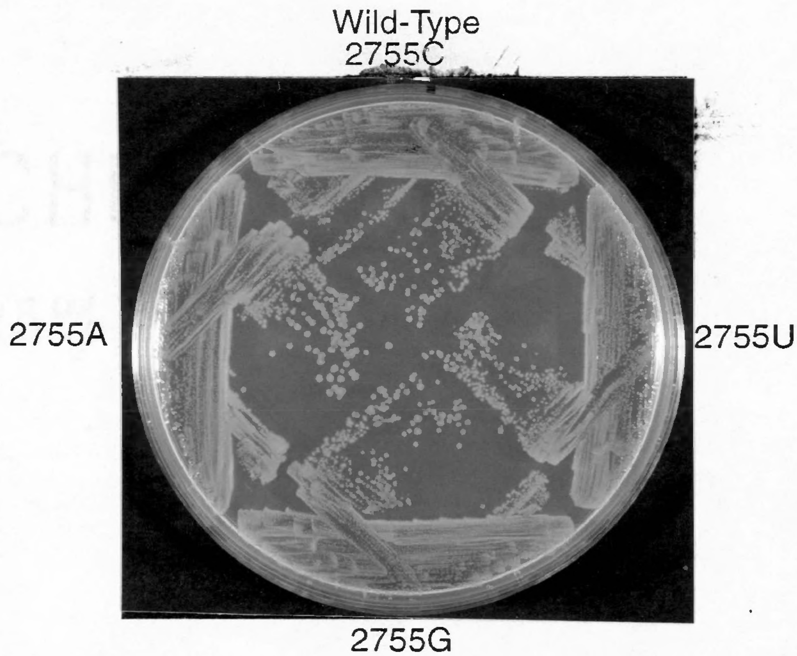

Figure 9. Growth of *E. coli* DH-1 cells containing pKK2755 single mutant constructs. Cells were grown on LB-amp^{200} solid media at 37°C for 24 hrs.

DH-1 cells and were termed lethal constructs: pKK791A-2755A, pKK791C-2755A, pKK791C-2755U, pKK791U-2755A, pKK791U-2755G and pKK791U-2755U.

The pKK791A-2755U construct was the most deleterious of those constructs that were viable in *E. coli* DH-1 cells. This double mutant resulted in colonies that grew at approximately one-third the rate of wild-type pKK3535 in DH-1 (Figure 10). The pKK791A-2755G double mutant produced colonies that grew slightly faster than the pKK791A-2755U double mutant (Figure 10). The pKK791C-2755G double mutant grew at approximately the same rate as wild-type in DH-1 (Figure 10).

Growth in 7-Deletion Strain

Seven-deletion strain cells were transformed with all single mutations at positions 2755 and 791 as well as with all double mutations at 791 and 2755. All of the single mutations at position 2755 (pKK2755A, G and U) were viable in the 7-deletion strain and the doubling times in LB at 37°C are reported in table 3. The following double-mutant constructs were not viable in the 7-deletion strain and were termed lethal: pKK791A-2755A, pKK791C-2755A, pKK791C-2755G, pKK791C-2755U, pKK791U-2755A and pKK791U-2755U. The three remaining double mutant constructs, 791A-2755G, 791A-2755U and 791U-2755G were viable in the 7-deletion strain and the doubling times in LB at 37°C are reported in table 3. These double mutant constructs are very interesting as all of the 791 single mutations (A, G and U) are lethal in the 7-deletion strain. These data show that the introduction of the second mutation at position 2755 are restoring viability to these constructs.

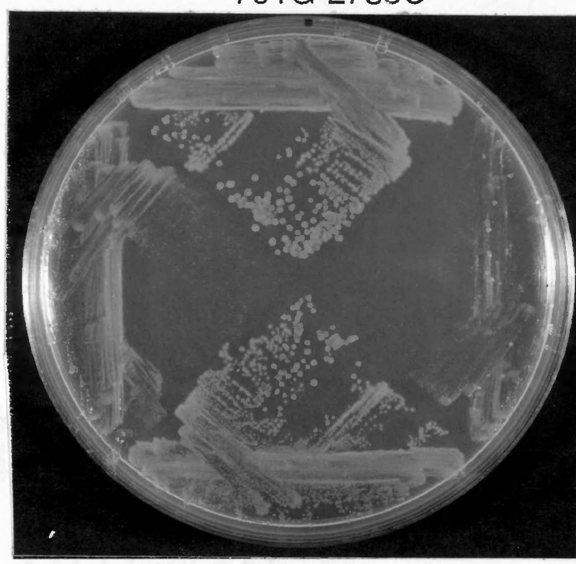

Figure 10. Growth of *E. coli* DH-1 cells containing pKK791-2755 double mutant constructs. Cells were grown on LB-amp^{200} solid media at 37°C for 24 hrs.

Table 3 Doubling times of 7-deletion strain cells containing pKK constructs.

Strain	**Doubling Time (min)**
pKK3535	54 ± 1
pKK2755A	52 ± 8
pKK2755G	43 ± 1
pKK2755U	59 ± 2
pKK791A-2755G	88 ± 2
pKK791A-2755U	83 ± 1
pKK791U-2755G	87 ± 7

Effects of rRNA Mutations *In Vitro*

Ribosomal Subunit Association Assays

DH-1

Ribosomes isolated from *E. coli* DH-1 cells were dialyzed in a buffer containing 1.5 mM $MgCl_2$ to completely dissociate ribosomes into 30*S* and 50*S* subunits. These free subunits were incubated in equimolar quantities in increasing amounts of $MgCl_2$ (6 and 10 mM) to monitor association affinity between the subunits (Figure 11). The subunit association profiles show that the purine transversion mutations (C to A and C to G) at position 2755 increase the association affinity between the mutant 50*S* subunits and wild-type 30*S* subunits as can be seen by the increased amount of 70*S* ribosomes compared to free 30*S* and 50*S* subunits. The opposite phenotype was seen for the C2755U transition mutation. This mutation gave rise to a noticeably lower affinity of mutant 50*S* subunits for wild-type 30*S* subunits even at the high $MgCl_2$ concentration. Profiles in Figure 11 are representative of repeated experiments yielding consistent results.

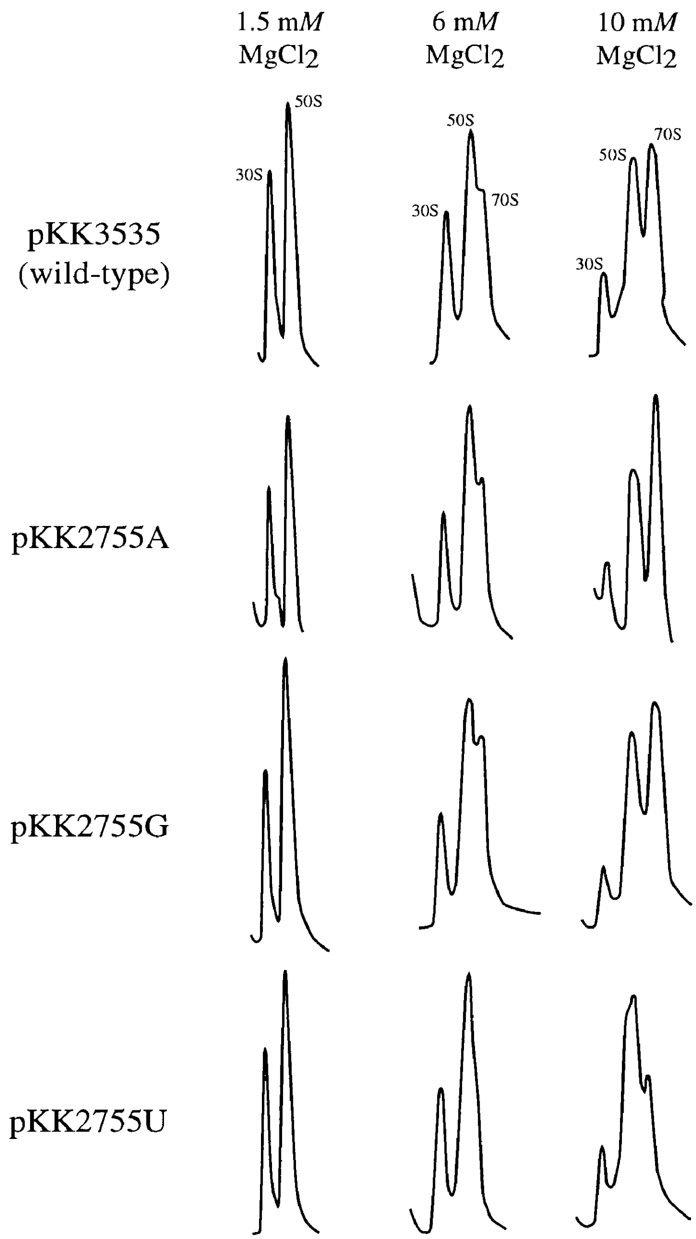

Figure 11. Subunit association profiles of ribosomes containing single mutations at position 2755 of 23*S* rRNA isolated from DH-1 cells. Ribosomal subunits were incubated in equimolar concentrations in increasing concentrations of $MgCl_2$ followed by centrifugation through a 5-30% sucrose gradient in a Beckman SW-41 rotor. 30*S*, 50*S* and 70*S* ribosomal peaks are marked.

7-Deletion Strain

Ribosomes were isolated from the 7-deletion strain, dialyzed and reassociated as described for the reassociation of ribosomes from DH-1 cells. The ribosome reassociation experiments for wild-type (2755C) and all three single mutants at position 2755 (A, G and U) shown in Figure 12 exhibit the same reassociation phenotype. These profiles show that the relative proportions of 30S, 50S and 70S peaks for each sample is the same.

The same assays were also done with ribosomes isolated from the three double mutants that were viable in the 7-deletion strain, 791A-2755G, 791A-2755U and 791U-2755G (Figure 13). These three double mutants each exhibit a greatly decreased association affinity compared to wild-type ribosomes, with the 791U-2755G mutant ribosomes showing the most deleterious association phenotype (Figure 13). Profiles in Figures 12 and 13 are representative of repeated experiments yielding consistent results.

Primer Extensions

Primer extension reactions were carried out on 16*S* and 23*S* rRNA isolated from wild-type and mutant ribosomal pools isolated from 7-deletion strain cells. The rRNA isolated from each mutant ribosomal pool was shown by the primer extension reactions to contain 100% mutant rRNA and no wild-type rRNA (data not shown).

Structure Probing

Structure probing of 70*S* ribosomes isolated from 7-deletion strain cells was done using DMS to identify structural changes caused by the rRNA mutations. All primer extension gels of rRNA isolated from chemically modified ribosomes are representatives of multiple experiments yielding consistent results. Figure 14 shows the gel of the primer extension reactions on modified rRNA isolated from the 2755 single mutant modification reactions; the differing intensities of the bands at position 2752C in the modified rRNA reactions are shown. As can be seen in Figure 14, the C2755A single mutation resulted in

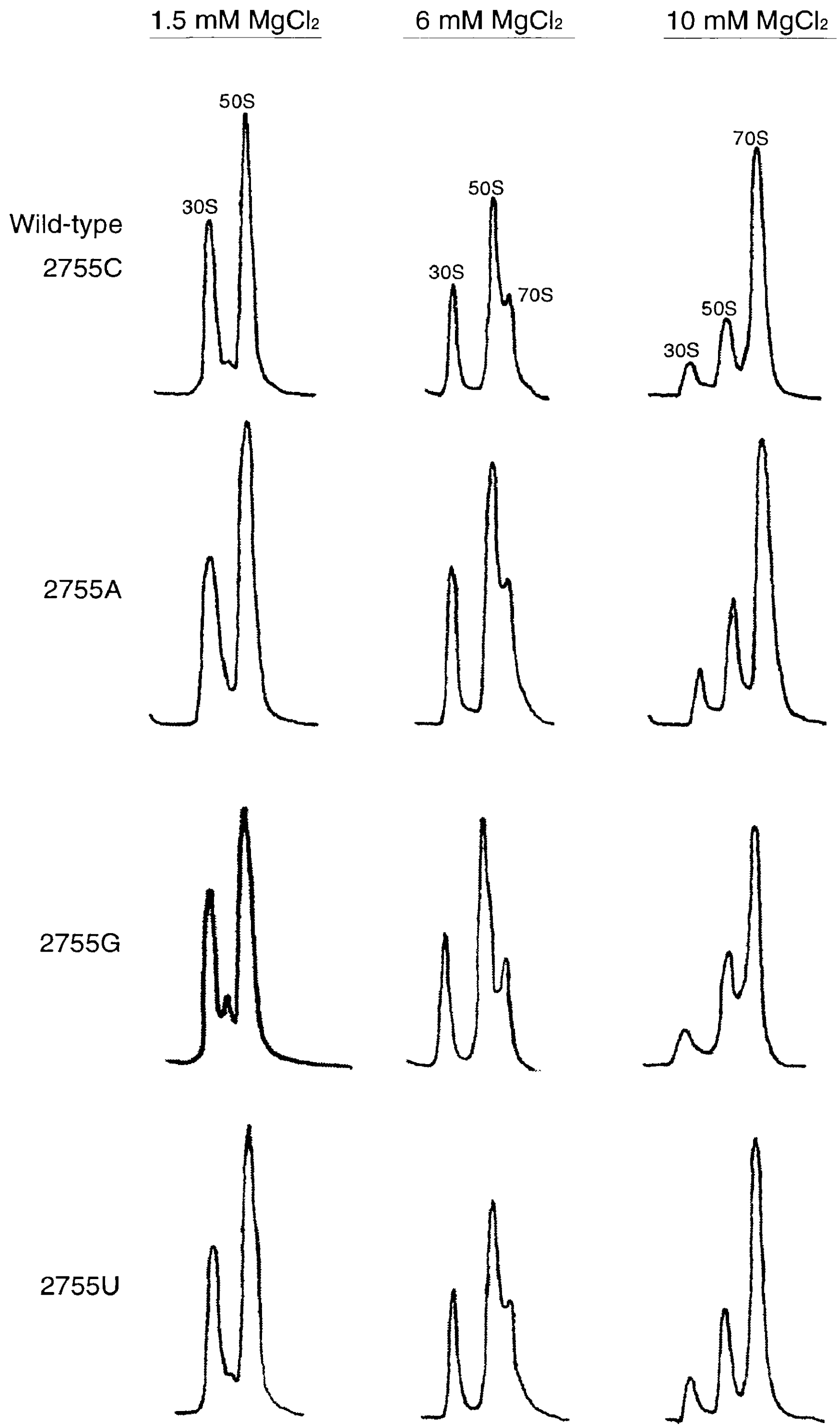

Figure 12. Subunit association profiles of ribosomes containing single mutations at position 2755 of 23*S* rRNA isolated from 7-deletion strain cells. Ribosomal subunits were incubated in equimolar concentrations in increasing concentrations of $MgCl_2$ followed by centrifugation through a 5-30% sucrose gradient in a Beckman SW-41 rotor. 30*S*, 50*S* and 70*S* ribosomal peaks are marked.

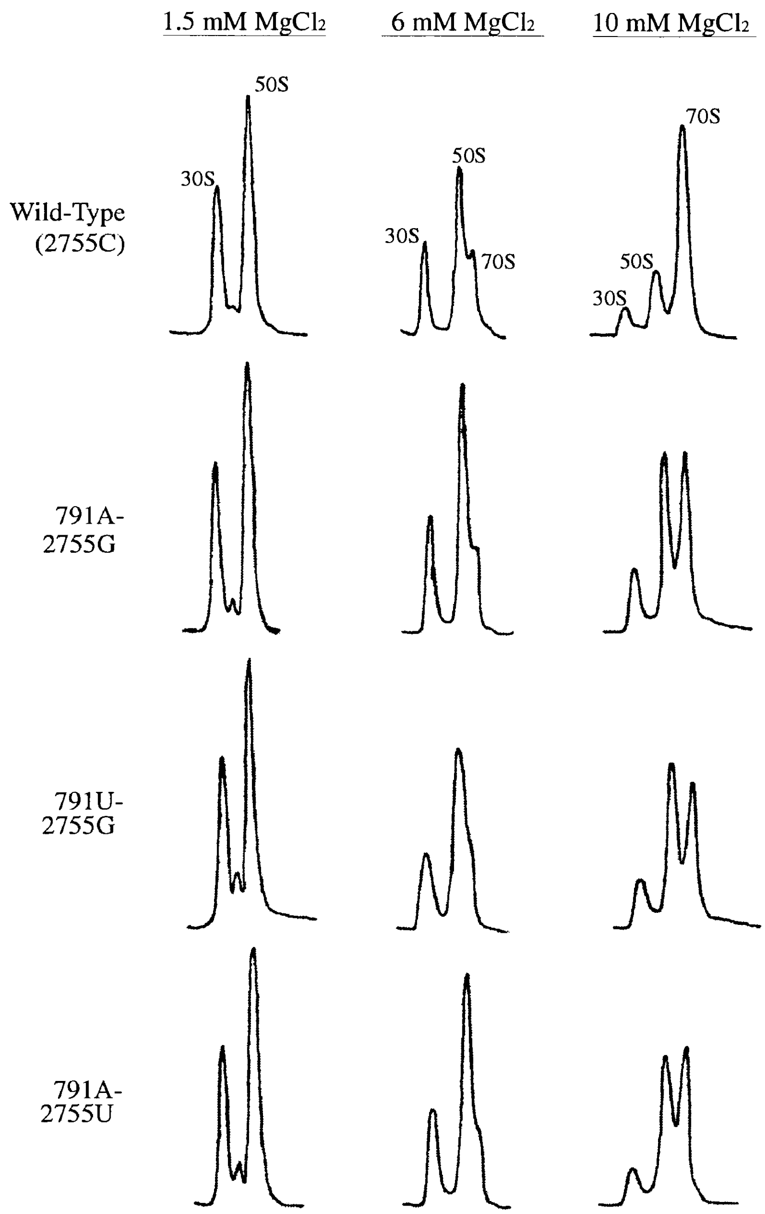

Figure 13. Subunit association profiles of ribosomes containing double mutations at positions 791 of 16*S* rRNA and 2755 of 23*S* rRNA isolated from 7-deletion strain cells. Ribosomal subunits were incubated in equimolar concentrations in increasing concentrations of $MgCl_2$ followed by centrifugation through a 5-30% sucrose gradient in a Beckman SW-41 rotor. 30*S*, 50*S* and 70*S* ribosomal peaks are marked.

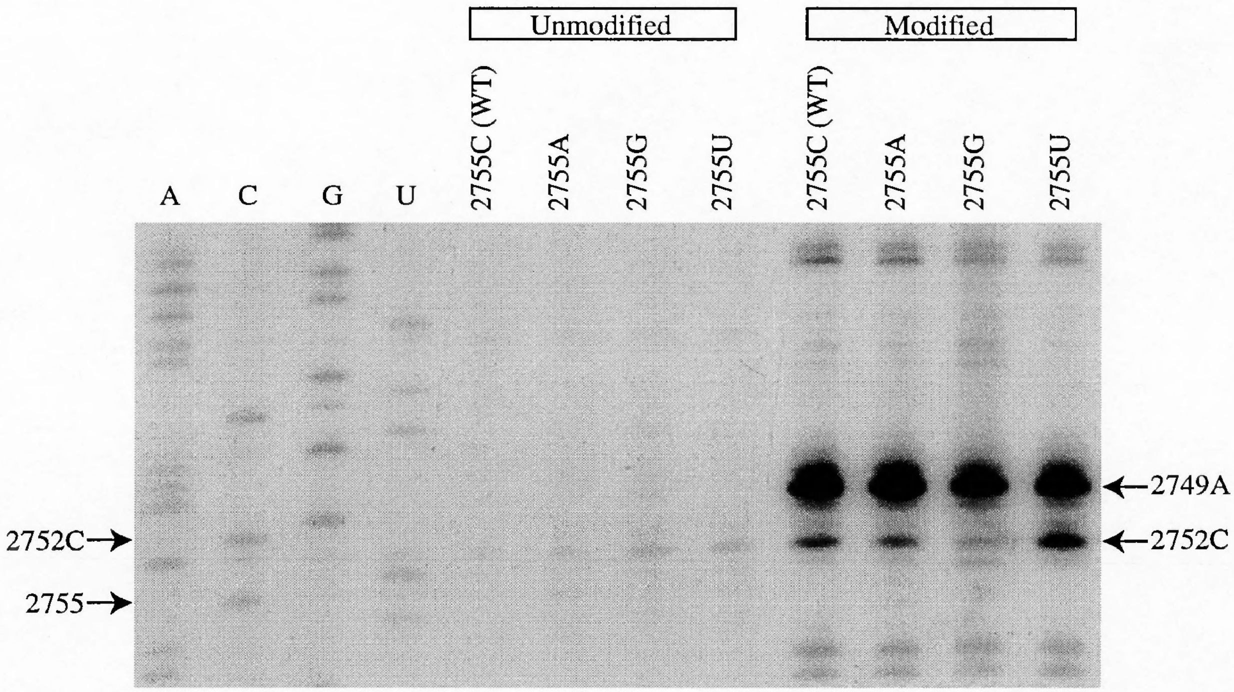

Figure 14. Polyacrylamide gel electrophoresis of primer extension reactions on rRNA isolated from DMS-modified 70*S* ribosomes containing single mutations at position 2755 of 23*S* rRNA. The 2750 region of 23*S* rRNA is probed. A, C, G and U lanes represent RNA sequencing lanes. Unmodified lanes indicate rRNA isolated from ribosomes carried through the modification reaction with the exception of the addition of DMS. Modified lanes indicate rRNA isolated from ribosomes modified with DMS.

the same modification pattern as wild-type when probing the 2750 region of 23*S* rRNA with the exception of a very slight protection of 2752C. The C2755G single mutation also exhibited the same modification pattern as wild-type with the exception of the protection of 2752C from modification with DMS (Figure 14). The C2755U single mutation shows the opposite effect of the previous two single mutations, resulting in an increased reactivity of 2752C (Figure 14). Figure 15 exhibits the results of primer extension reactions probing the 790 region of the 16*S* rRNA isolated from the modified ribosomes with single mutations at position 2755. This gel shows that all three of the single mutants at position 2755 exhibit the same modification pattern in the 790 region as wild-type.

DMS modified ribosomes containing the 791A-2755G and 791U-2755G double mutants showed protections of 2752C when probing the 2750 region and enhancement of reactivities of 789U, 790A, 791 (A and U), 792A, 794A and 795C when probed for the 790 region (Figure 16). The 791U-2755A double mutant showed no differences in modification when probing the 2750 region, however, this double mutant exhibited the same modification pattern of the 790 region as described for the two previous double mutants (Figure 16). The reactivities of nucleotides 789U and 791U provide a very puzzling result as uracil has not been shown capable of being modified with DMS.

To verify that the differences in reactivities seen in the double mutant reactions were not attributable to free 30*S* subunits in the reactions, structure probing was also done on free 30*S* ribosomal subunits containing wild-type 791G as well as 30S subunits containing the A and U mutants at position 791. These subunits were isolated from the double mutant ribosomal pools and the resultant gel is shown in Figure 17. The reactions presented in this figure show that the modification patterns of the mutants at position 791 were the same as wild-type with the exception of the increase in reactivity of nucleotide 791 in the two mutant samples. Again, the unusual modification of 791U by DMS is present.

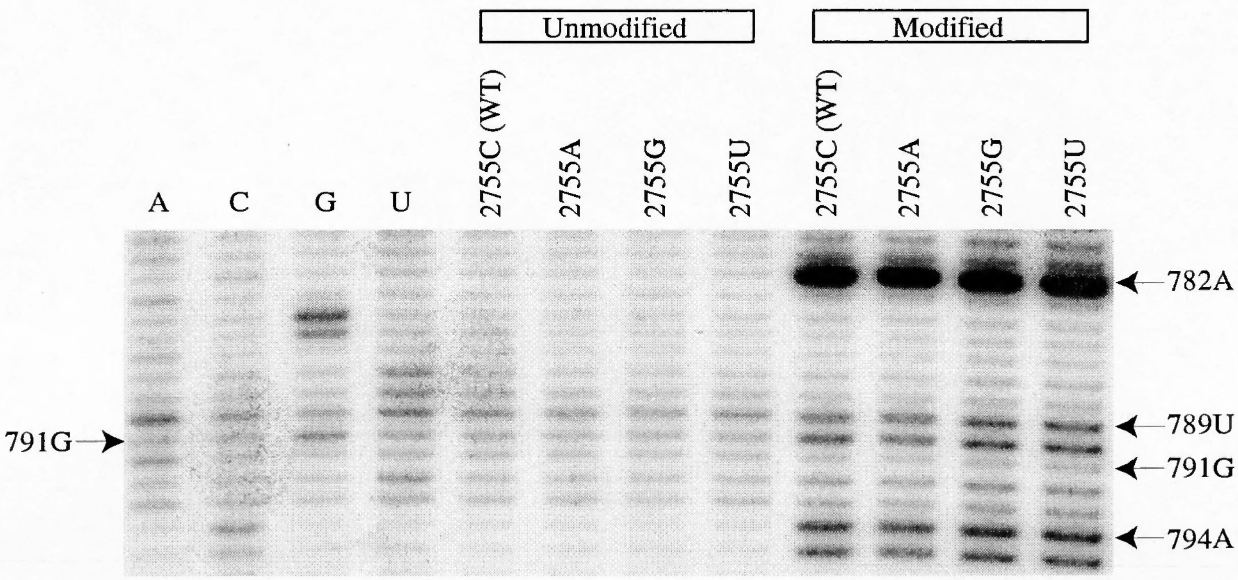

Figure 15. Polyacrylamide gel electrophoresis of primer extension reactions on rRNA isolated from DMS-modified 70*S* ribosomes containing single mutations at position 2755 of 23*S* rRNA. The 790 region of 16*S* rRNA is probed. A, C, G and U lanes represent RNA sequencing lanes. Unmodified lanes indicate rRNA isolated from ribosomes carried through the modification reaction with the exception of the addition of DMS. Modified lanes indicate rRNA isolated from ribosomes modified with DMS.

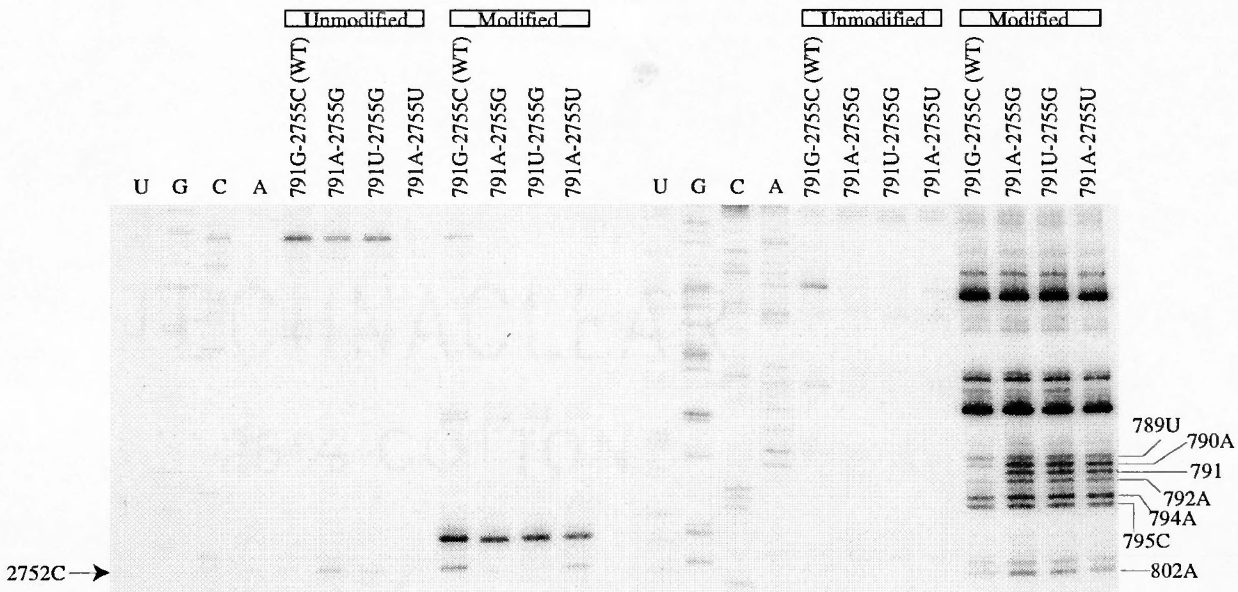

Figure 16. Polyacrylamide gel electrophoresis of primer extension reactions on rRNA isolated from DMS-modified 70*S* ribosomes containing double mutations at positions 791 of 16*S* rRNA and 2755 of 23*S* rRNA. The 790 region of 16*S* rRNA and the 2750 region of 23S rRNA are probed. A, C, G and U lanes represent RNA sequencing lanes. Unmodified lanes indicate rRNA isolated from ribosomes carried through the modification reaction with the exception of the addition of DMS. Modified lanes indicate rRNA isolated from ribosomes modified with DMS.

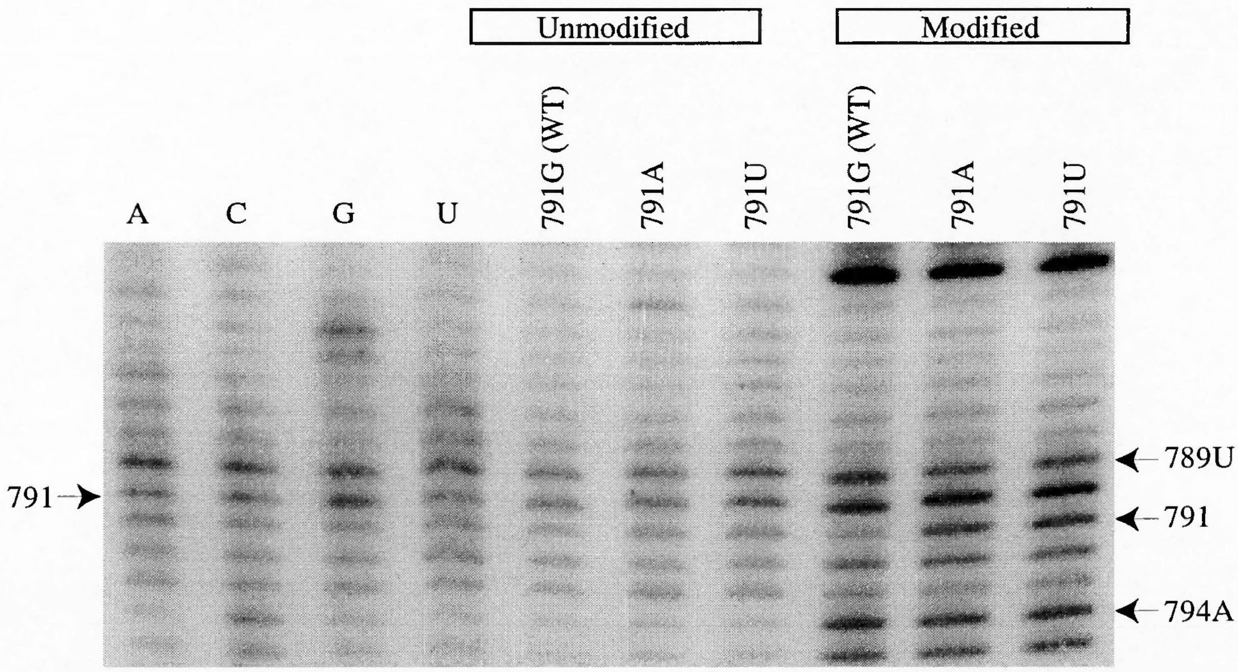

Figure 17. Polyacrylamide gel electrophoresis of primer extension reactions on rRNA isolated from DMS-modified 30*S* ribosomal subunits containing single mutations at position 791 of 16*S* rRNA. 790 region of 16*S* rRNA is probed. A, C, G and U lanes represent RNA sequencing lanes. Unmodified lanes indicate rRNA isolated from 30*S* ribosomal subunits carried through the modification reaction with the exception of the addition of DMS. Modified lanes indicate rRNA isolated from 30*S* ribosomal subunits modified with DMS.

Chapter 4. Discussion

Subunit association is one of the most important features of translation. Since the events of mRNA decoding occur on the small subunit and peptide bond formation on the large subunit it is impossible for protein synthesis to proceed without association. Recently it has become clear that the interacitons between the large and small ribosomal subunits are more complex than a single association event. As tRNAs traverse the ribosomal binding sites, they occupy new positions on one subunit while remaining stationary on the other (Moazed & Noller, 1989). Such intermediate states of tRNA movement imply relative motion between the two subunits (Wilson & Noller, 1998a). It has been suggested that the necessity of such relative movement explains the universally conserved two subunit structure of the ribosome (Wilson & Noller, 1998b). This implies that the ribosomal subunits adopt multiple association states, each of which must be characterized by unique sets of subunit-subunit interactions. These interactions must be stable enough to lock the associated ribosome into a particular functional state, while also retaining the ability for dynamic change. As with most ribosomal activities, it is likely that rRNA provides many of the critical interactions for these subunit association states.

The overall objective of this study was to evaluate the role of the 2750 loop of *E. coli* 23*S* rRNA in subunit association (see Figure 4). Previous work has suggested that the nucleotides in this loop are important for the association process (Hill et al., 1988; Herr et al., 1979). Since a six nucleotide region of this loop is complementary to a region of 16*S* rRNA also proven to be critical for association, a simple base-pairing model has been proposed (see Figure 4; Herr et al., 1979). It was also the purpose of this study to investigate the validity of this base-pairing model.

A wealth of data has been generated describing the location of the 790 loop of 16*S* rRNA within the 30*S* subunit of the ribosome. Chemical modification data along with oligonucleotide directed probing have provided evidence that this loop is located on the surface of the 30*S* subunit and at the interface between the 30*S* and 50*S* subunits (Chapman & Noller, 1977; Tapprich & Hill, 1986). A three dimentional model of the 30*S* subunit based on these data has placed the 790 loop on the upper portion of the platform near the cleft of the subunit (Noller et al., 1987). Much less evidence has been provided to detail the location of the 2750 loop of 23*S* rRNA within the 50*S* subunit. Earlier work by Noller's group and more recent modeling by Brimacombe's group have placed the 2660 loop near the interface with the 30*S* subunit and this loop is a close neighbor of the 2750 loop (Moazed et al., 1988; Brimacombe, 1995). Along with the oligonucleotide probing work (Hill et al., 1988), this study gives strong evidence that the 2750 loop is at the interface of the two ribosomal subunits.

Site-directed mutagenesis is a powerful method for testing the functional capabilities of rRNA (Tapprich et al., 1990). For the evaluation of base-pairing, compensatory mutagenesis offers a direct approach (Vila et al., 1994). This mutagenic approach was utilized for the evaluation of the 2750 loop. Position 2755C was mutated to 2755A, 2755G and 2755U. Potential compensatory mutations at position 791 in 16*S* rRNA were constructed to evaluate the possibility of base-pairing between 16*S* and 23*S* rRNA. Table 4 represents a brief summary of data obtained in this study concerning all of the mutant constructs and is meant to be used as a reference while reading this chapter. Together, the results of studying the single mutants at positions 2755 and 791 as well as the double mutants indicate that each region is involved in ribosomal subunit association. In addition, it is clear from the results of the double mutants that the structure of the 2750 loop has an influence on both the structure and the function of the 790 loop and that in the case of the 791A-2755U double mutant the 790 loop influences the structure and function of the 2750 loop. However, it does not appear likely that simple base-pairing is adequate to explain the molecular mechanism of this influence. Initially, the 2755 mutants were evaluated in DH-1 cells and the results suggest that the single mutations have little, or no, obvious effect on

Table 4. Summary of growth, association, and chemical modification data. This table provides a brief summary of data from this study to be used as a reference for the discussion section. Growth characteristics of DH-1, subunit association characteristics from DH-1 and the 7-deletion strain, and DMS modification data from the 7-deletion strain are described using a "+" system. Increased numbers of "+'s" represent increases in each of the characteristics measured. Doubling times of 7-deletion strain cells are measured in minutes. Abbreviations used in the table include: 7-del = 7-deletion, L = lethal, N.A. = not applicable, N.D. = experiment was not done.

	Growth		Association		DMS Modification (7-Deletion Strain)		
Construct	DH-1	7Del	DH-1	7Del	2752C	790 Loop	30*S* Subunit
pKK3535	++++	54±1	+++	++++	++	+	+
pKK2755A	++++	52±8	++++	++++	++	+	N.A.
pKK2755 G	++++	43±1	+++	++++	+	+	N.A.
pKK2755 U	+++	59±2	+	++++	+++	+	N.A.
pKK791A	++	L	+	L	L	L	N.A.
pKK791C	L	L	L	L	L	L	N.A.
pKK791U	+	L	N.D.	L	L	L	N.A.
pKK791A-2755A	L	L	L	L	L	L	N.A.
pKK791A-2755G	++	88±2	N.D.	++	+-	+++	++
pKK791A-2755U	++	83±1	N.D.	++	++	+++	N.D.
pKK791C-2755A	L	L	L	L	L	L	L
pKK791C-2755G	++++	L	N.D.	L	L	L	L
pKK791C-2755U	L	L	L	L	L	L	L
pKK791U-2755A	L	L	L	L	L	L	L
pKK791U-2755G	L	87±7	L	++	+	+++	++
pKK791U-2755U	L	L	L	L	L	L	L

translation *in vivo*. The effects of the single mutations at position 2755 (pKK2755A, G and U) on growth in DH-1 cells are shown in Figure 9. It is clearly seen that the growth characteristics of each of the 2755 single mutants are essentially the same as cells containing the wild-type plasmid (pKK3535) with the exception of pKK2755U, which is slightly slower.

The growth characteristics of the combination mutations present a much different scenario than the single mutants (Figure 10). The introduction of the 791A mutation in combination with the 2755G mutation is viable in DH-1, yet bestows a very deleterious effect on cell growth. This result suggests that the 791A mutation is the major contributor in the deleterious effect on growth since the 2755G mutation alone does not confer a noticeable alteration in cell growth. The notion that the 791A mutation is the major contributor to the deleterious growth phenotype is substantiated by a previous study showing the deleterious growth effect of the 791A single mutation (Tapprich et al., 1989). The 791A-2755U combination mutation presents an even more deleterious effect on growth than the 791A-2755G combination mutation. The slow growth of this combination mutant suggests that the 2755U mutation which, by itself, is slightly slower than wild-type enhances the deleterious effect of 791A. This result is inconsistent with the simple Watson-Crick base-pairing model proposed for positions 791 and 2755 (see Figure 4 for review). It is unlikely that the loss of one hydrogen bond in the center of the duplex would have a major effect on cell growth. Taken together, these results suggest that the slow growth of these double mutants is not likely to represent a direct interaction between 791 and 2755.

In contrast to the combination mutations involving 791A, the 791C-2755G double mutation confers growth characteristics essentially equal to those of wild-type. This is a very interesting result because the 791C single mutation is lethal in DH-1. The complete recovery of growth to that of wild-type presents the possibility that the reversal of a potential G-C base-pair to a C-G base-pair between positions 791 and 2755 restores wild-type function to the mutant ribosomes. Although this result fits the base-pairing model precisely, the 791A-2755U growth results together with the lethality of the other potential base-paired constructs (791U-2755A, 791U-2755G), make this hypothesis unlikely. Nevertheless, the 2755G mutation must influence the structure and function of the ribosome in some way, perhaps by stabilizing a structure required for efficient translation.

The recent availability of a strain lacking all chromosomal rRNA operons has allowed for the study of pure populations of mutant ribosomes. Surprisingly, some rRNA mutants described in this study behave radically different when present in the absence of wild-type ribosomes. The doubling times of the 2755 single mutations in the 7-deletion strain (Table 3) exhibit moderate differences. The 2755A and U mutations confer growth rates essentially the same as wild-type while the 2755G mutant displays an eleven minute faster doubling time. It is interesting to note that the 2755G mutation enabled two lethal mutants (791A and 791U) to grow in the 7-deletion strain. The 2755G mutation also enabled the lethal mutant 791C to grow in DH-1 (but not in the 7-deletion strain). Clearly, the 2755G mutation had a profound effect on the ribosome.

Each of the 791 single mutations are lethal in the 7-deletion strain, indicating serious defects in protein synthesis. Intriguingly, when the 791A and 791U mutations are present in the double mutant constructs 791A-2755G, 791A-2755U and 791U-2755G, cell viability is rescued, albeit with substantially slower than wild-type doubling times (Table 3). These data suggest that the 2755 mutations are offsetting the deleterious effects of the 791 single mutations enough to restore viability. A surprising result is the lethality of the 791C-2755G combination mutant in the 7-deletion strain. As stated above, 2755G rescues the lethal phenotype of 791C in DH-1 cells, which also contain wild-type ribosomes, and confers cell growth nearly equal to wild-type. Once again, this result argues against a simple Watson-Crick base-pairing model between the 790 and 2750 loops since the reversal of a G-C base-pair to a C-G base-pair in the proposed RNA duplex should not interfere with its stability. Alternatively, it seems that the structure adopted by 2755 mutants altered the structure of 791 mutants sufficiently to restore a low level of functionality to the ribosome. Such interaction between 791 and 2755 is likely to involve allosteric conformational changes. It has been shown previously that position 791 undergoes allosteric changes (Moazed & Noller, 1987). This base, together with positions 790, 909, 1394, 1413 and 1487, belongs to the so-called class III sites. These sites are protected from chemical probes by tRNA, 50*S* subunits, and antibiotics, all of which can bind simultaneously to 30*S* subunits (Moazed & Noller, 1986). This behavior provides evidence for allosteric changes in rRNA and reinforces the importance of subunit association in tRNA interactions (Noller et al., 1990).

The *in vitro* reassociation assays of ribosomes isolated from DH-1 cells containing single mutations at position 2755 (Figure 11) display association phenotypes which appear to be somewhat at odds with the growth characteristics of the mutants (Figure 9). The 2755A and G purine substitutions result in the 50*S* subunits acquiring a higher association affinity for wild-type 30*S* subunits compared to wild-type 50*S* subunits. These results are only the second instance in which an increase in association affinity has been observed (Staplin, 1995).

While the 2755A and G purine substitutions enhanced subunit affinity, the 2755U transition mutation resulted in greatly diminished association between mutant 50*S* subunits and wild-type 30*S* subunits. The growth of these cells is only slightly slower than wild-type, yet *in vitro* reassociation assays clearly show that affinity between the subunits is substantially decreased. It should be noted that *in vitro* subunit association assays are very different from translation *in vivo*. During the association assay the subunits are devoid of factors, tRNAs and mRNA, all of which contribute to the affinity of 30*S* subunits for 50*S* subunits in the translation cycle. For the *in vitro* assay, only those interactions that make direct subunit-subunit contact are tested. In the cell, it is likely that other ligands are able to compensate for the effects of the 2755 mutations on subunit-subunit affinity.

The *in vitro* reassociation assays of 2755 single mutant ribosomes isolated from 7-deletion strain cells all exhibit profiles essentially identical to the wild-type profiles (Figure 12). These results show that the 2755 single mutations are not affecting subunit association *in vitro* and correlate well with their respective growth rates in the 7-deletion strain (Table 3). The differences in reassociation profiles for the 2755 single mutants in DH-1 and the 7-deletion strain do not make for easy interpretation. There were several instances during this study where the results in DH-1 differed from the results in the 7-deletion strain. This issue is addressed more completely below.

The *in vitro* reassociation assays of the 791-2755 double mutant ribosomes demonstrate a marked decrease in subunit association (Figure 13). For the most part, these association defects seem to be attributable to the mutations at position 791, since the association profiles of the 2755 single mutations mirror those of wild-type in the 7-deletion strain. However, the results of DMS-modification experiments also suggest that 2755 mutations alter the structure of the 791 region and vice versa. Thus the influences of each mutation on subunit association and growth may be quite complex. Overall, increases in cell doubling time correlate with decreases in subunit association. This indicates that a decrease in subunit association is either directly or indirectly responsible for the slow growth phenotypes. Reassociation studies were not done with double mutant ribosomes isolated from DH-1 cells.

A much clearer picture of the effects of rRNA mutations is provided by the 7-deletion strain. Primer extension reactions on rRNA extracted from mutant ribosomes isolated from 7-deletion strain cells revealed ribosome populations that were 100% mutant (data not shown). Such homogeneous populations undoubtedly result in more accurate accounts of ribosome structure and function due to the absence of interfering wild-type ribosomes. For that reason, the results of studies in the 7-deletion strain should be viewed with greater confidence. However, not all experiments are possible in the 7-deletion strain. As indicated in this study, only six of the fifteen possible mutant combinations at 791 and 2755 were viable in the 7-deletion strain. The characteristics of the remaining nine combinations could not be observed.

Ribosomes containing the 2755 single mutations were modified using DMS and changes in the accessibility of position 2752C to the modifying reagent were observed (Figure 14). When 2755C is mutated to 2755G the 2750 loop is altered in such a way that position 2752C is no longer accessible to DMS. When 2755C is mutated to 2755U the opposite effect is seen. In this case, the accessibility of DMS to position 2752C is enhanced. These data show that structural changes are occurring within or near the 2750 loop. Furthermore, different base identities lead to different structural alterations. These are assumed to be subtle changes as they do not appear to affect either growth or association phenotypes. The 790 region of rRNA from these 2755 single mutant ribosomes was also probed and showed no differences in modification. The single mutations at position 2755 did not affect the structure of the 790 region in 70*S* ribosomes (Figure 15).

Ribosomes containing the 791-2755 combination mutations provided exciting results when analyzed by DMS modification (Figure 16). These mutations provided the clearest evidence that structural changes in the 2750 region of 23*S* rRNA caused conformational alterations in the 790 region of 16*S* rRNA and vice versa. For the 791A-2755G and 791U-2755G double mutants, 2752C was protected from DMS modification. These protections are probably attributable to the 2755G mutation as this same effect is seen in the absence of the 791U mutation (Figure 14). A more dramatic indication of structural changes across the subunit interface is seen with the 791A-2755U combination mutation. The 2755U single mutation resulted in a large enhancement of DMS modification at position 2752C. This reactivity is reduced to the level of wild-type when the 791A mutation is combined with 2755U. The restoration of reactivity to that of wild-type may be due to a conformational change of the 2750 loop in which the 791A mutation influences the loop to adopt a conformation similar to wild-type. Such a conformational restoration may be the reason that the lethal 791A mutant is able to survive when combined with 2755U.

More dramatic effects of these combination mutations on rRNA structure is seen when the 790 loop is probed (Figure 16). Each of the double mutants (791A-2755G, 791A-2755U and 791U-2755G) result in an immense increase in the reactivities of nucleotides 790A, 791A and U (depending upon the mutation present at position 791), and 792A. These positions have previously been shown to be protected in 70*S* ribosomes (Chapman & Noller, 1977; Moazed & Noller, 1986; Moazed & Noller, 1990; Herr, Chapman & Noller, 1979). Subtle increases in reactivity are also observed in the double mutants at positions 794A and 795C which are also normally protected in 70*S* ribosomes (Moazed & Noller, 1990). In contrast to the variable structural alterations noted for the 2750 loop in the 791-2755 combination mutants, the structural changes in the 790 loop are very consistent. In each case the nucleotides between 789 and 792 become exposed and positions 794 and 795 become slightly exposed. This is a very significant finding. Previous studies have shown that these nucleotides are protected from modification upon subunit association (Chapman & Noller, 1977; Moazed & Noller, 1986; Moazed & Noller, 1990). This was confirmed in the wild-type control experiment shown in figure 16. Studies have also shown that conformational alterations in the 790 loop are likely to define the various functional states of the ribosome (Moazed & Noller, 1987). As outlined above, the behavior of the class III bases in the 790 loop suggest that the function of the loop is allosterically regulated. The fact that 2755 mutations induce the exposed state in the 790 loop suggest that an interaction involving the 30*S* subunit and the 2750 loop may trigger allosteric changes in the 790 loop during translation. Thus an interaction between the 2750 loop in 23*S* rRNA and the 790 loop in 16*S* rRNA is critical for subunit association. Rather than occurring through direct Watson-Crick base-pairing, the evidence provided by this study indicates that the interaction is allosteric in nature. A precedence for a conformational change within the ribosome has been set (Lodmell & Dahlberg, 1997).

One potential explanation for the exposure of 790 loop nucleotides in the double mutants was simply an increase in free 30*S* subunits. Several positions in the 790 loop are more reactive (more exposed) in free 30*S* subunits than in 70*S* ribosomes. Figure 13 shows that the amount of free 30S subunits in the ribosome preparation from the double mutants is likely to be greater than that found in wild-type ribosome preparations.

To make sure that these observed increases in modification within the 790 loop were not attributable to a simple increase in free 30*S* subunits in the preparation, 30*S* subunits containing the 791A and 791U mutations were modified with DMS in the absence of 50*S* subunits (Figure 17). The results of this experiment reveal that free 30S subunits, whether wild-type or mutant, do show an increased DMS modification at positions 789, 790 and 792 as previously described (Chapman & Noller, 1977; Moazed & Noller, 1986). However, the level of increase is much less than that observed in the double mutant preparation shown in figure 16. Furthermore, the free 30*S* subunits do not show enhanced reactivity at positions 794 and 795. Also note that the reactivity of 791A in the mutant 30*S* subunit modification is enhanced while wild-type (791G) is not. This is due to the fact that G is reactive to DMS at N7 but does not inhibit reverse transcriptase while A is reactive at N1 and this modification does inhibit reverse transcriptase, thus the seemingly dramatic increase in reactivity. This result further substantiates the claim that position 791 is located on the surface of the 30*S* subunit as shown previously (Chapman & Noller, 1977; Tapprich & Hill, 1986). Uracil has not previously been shown to be modified with DMS, therefore, the increase in reactivity at 791 in the 30*S* subunits containing 791U is not easily explained and is addressed below. Together, the results clearly support the model suggesting that mutations at position 2755 alter the structure of nucleotides in the 790 loop.

It is somewhat troubling that position 791 becomes modified at all in the free mutant 30*S* subunits as well as in the 791U-2755A mutant 70*S* ribosomes. The chemistry of DMS modification suggests that the only reactive positions are N1 of A, N3 of C, and N7 of G (Ehresmann et al., 1987). Yet 791U is clearly modified in the 791U-2755A sample and in the free 30*S* subunit (Figures 16, 17). At present, there is no clear explanation for this anomolous modification. Perhaps the structure of the 790 loop has placed 791U into an environment where N3 becomes reactive. If so, this result emphasizes the dramatic structural perturbation found in the 791U-2755A double mutant ribosomes.

During the course of this study there were many examples where results obtained from DH-1 are not completely consistent with those obtained from the 7-deletion strain. For example, the 791C-2755G mutant was viable in DH-1 but not the 7-deletion strain, whereas the 791U-2755G mutant was viable in the 7-deletion strain and not in DH-1. In addition, there were differences in subunit association assays for the 2755 single mutants when the ribosomes were derived from DH-1 but there were no differences when the ribosomes were derived from the 7-deletion strain. There is currently no reliable explanation for these observed differences. With the seven chromosomal rRNA operons deleted, there may be differences in expression from the chromosome and possibly differences in the overall physiology of the cell which may contribute to differences seen in this 7-deletion strain. The way that mixed populations of wild-type and mutant ribosomes interact in comparison to pure populations of mutant ribosomes has also not been detailed. For the double mutants in DH-1, the number of combinations of interacting subunits is quite complex. Given the differences observed for DH-1 results and 7-deletion strain results, it would seem that one or more of these combinations has an overwhelming effect on the function of the ribosomes.

The largest inconsistency observed between these two strains has been the 791C-2755G double mutant which rescues the lethal 791C single mutant in DH-1, but is lethal in the 7-deletion strain. One potential explanation for these results involves the affinity of mutant 30*S* subunits for IF3. It has been shown that 30*S* subunits containing 791A have a lowered affinity for IF3 (Tapprich et al., 1989) and it is possible that the 791C mutation results in an increased affinity. It is estimated that intracellular concentrations of IF3 are 10-fold lower than that of ribosomes and that nearly all IF3 in the cell is bound to native 30*S* subunits (Gualerzi & Pon, 1990). Based on these data, it is possible that 30*S* subunits containing 791C are sequestering IF3 within the cell. This would result in depleted levels of IF3 and premature binding of 50*S* subunits to 30*S* subunits inhibiting the proper formation of the 30*S* initiation complex. It is also possible that the 2755G mutation confers an increased affinity of 50*S* subunits containing the mutation for the mutant 30*S* subunits. If this is the case, this increased affinity may result in mutant 50*S* subunits competing with IF3 for mutant 30*S* subunits, or even displacing IF3 from these subunits, thus restoring a viable intracellular concentration of IF3. If this is indeed the case, the explanation for lethality in the 7-deletion strain is elementary. The increased affinity between the mutant 30*S* and 50*S* subunits does not allow for the formation of the 30*S* initiation complex and thus does not allow for translation. Two experiments may be done to test this hypothesis. First, a binding study could be done using a pure population of 50*S* subunits containing the 2755G mutation isolated from the 7-deletion strain and a mixed population of 30*S* subunits isolated from the 791C-2755G double mutant in DH-1. This assay would determine if an increased affinity of mutant 50*S* subunits for mutant 30*S* subunits exists. A second binding study involving IF3 could also be used to test the hypothesis. This study would involve isolating 30*S* subunits from the double mutant in DH-1 and determining whether there was a difference in affinity between the mutant and wild-type subunits for IF3.

When taken together, the results of this study indicate that the 790 loop of 16*S* rRNA and the 2750 loop of 23*S* rRNA are not interacting by simple Watson-Crick base-pairing. It is clearly shown that subtle differences in DMS modification within the 2750 loop result from mutations at position 2755. These single mutations most likely confer a structural change within the 2750 loop, however, they do not induce a change across the subunit in the 790 loop or have a major affect on subunit association (in the 7-deletion strain) or on cell growth.

The viable double mutants in the 7-deletion strain have a much greater effect on ribosome structure, subunit association and cell growth. These mutants have very deleterious effects on cell growth and subunit association. The most notable effect of these mutants is the effect on the structure of rRNA within the 790 and 2750 loops in 70*S* ribosomes. The introduction of the 2755G and U mutations rescue lethal 791A and U single mutants. It is proposed that the mutations at position 2755 allow the 2750 loop to interact with the 790 loop mutant at position 791. This interaction involves the mutant 2750 loop conferring a conformational change across the ribosomal subunits to the mutant 790 loop, converting the 790 loop to a more exposed structure. The subsequent exposure allows for the improved function of the ribosomes, such that translation levels are sufficient to support growth.

To more completely detail the complex nature of the 790 and 2750 loops, numerous additional experiments must be completed. Additional reassociation experiments may be performed using 30*S* subunits isolated from double mutants in the 7-deletion strain containing the 791A and 791U mutations. These subunits may be reassociated with wild-type 50*S* subunits as well as with 50*S* subunits containing the 2755A and 2755U mutations, allowing *in vitro* association assays of lethal constructs. Polyribosome preparations of the viable mutations in the 7-deletion strain as well as the 791C-2755G construct in DH-1 should be done to illustrate the *in vivo* characteristics of the mutant ribosomes. To more thoroughly explore the structure and function of other nucleotides within and surrounding the 790 and 2750 loops, additional chemical modification experiments employing ß-ethoxy-∝-ketobutyraldehyde (kethoxal), 1-cyclohexyl-3-(2-morpholinoethyl)-carbodiimide metho-*p*-toluene sulfonate (CMCT), DMS-N7 (aniline cleavage), and diethylpyrocarbonate (DEPC) are required. Lastly, tRNA binding studies using pure populations of ribosomes containing mutations at position 791 would provide more information important for the understanding of the intricate structure and function of the ribosome.

Literature Cited

Agrawal, R.D. and Burma, D.P. 1996. Sites of ribosomal RNAs involved in the subunit association of tight and loose couple ribosomes. J. Biol. Chem. 271 (35): 21285-21291.

Bretscher, M.S. 1968. Translocation in protein synthesis: a hybrid structure model. Nature. 218: 675-677.

Brimacombe, R. 1995. The structure of ribosomal RNA: a three-dimensional jigsaw puzzle. Eur. J. Biochem. 230: 365-383.

Brosius, J., Ullrich, A., Raker, M.A., Gray, A., Dull, T.J., Gutell, R.R. and Noller, H.F. 1981. Construction and fine mapping of recombinant plasmids containing the *rrnB* ribosomal RNA operon of *E. coli.* Plasmid. 6: 112-118.

Chapman, N.M. and Noller, H.F. 1977. Protection of specific sites in 16*S* RNA from chemical modification by association of 30*S* and 50*S* ribosomes. J. Mol. Biol. 109: 131-149.

Egebjerg, J., Larsen, N. and Garrett, R.A. 1990. In Hill, W.E., Dahlberg, A.E., Garrett, R.A., Moore, P.B., Schlessinger, D. and Warner, J.R. (eds), *The Ribosome: Structure, Function and Evolution.* Amer. Soc. Microbiol., Washington, D.C., pp. 168-179.

Ehresmann, C., Baudin, F., Mougel, M., Romby, P., Ebel, J-P. and Ehresmann, B. 1987. Probing the structure of RNAs in solution. Nucl. Acids Res. 15 (22): 9109-9128.

Firpo, M.A. and Dahlberg, A.E. 1998. The importance of base pairing in the penultimate stem of *Escherichia coli* 16*S* rRNA for ribosomal subunit association. Nucleic Acids Res. 26 (9): 2156-2160.

Firpo, M.A., Connelly, M.B., Goss, D.J., and Dahlberg, A.E. 1996. Mutations at two invariant nucleotides in the 3'-minor domain of Escherichia coli 16*S* rRNA affecting translational initiation and initiation facor 3 function. J. Biol. Chem. 271 (9): 4693-4698.

Gualerzi, C.O. and Pon, C.L. 1990. Initiation of mRNA translation in prokaryotes. Biochemistry 29 (25): 5881-5889.

Gutell, R.R., Larsen, N., Woese, C.R. 1994. Lessons from an evolving rRNA: 16*S* and 23*S* rRNA structures from a comparative perspective. Microbiol. Rev. 58 (1): 10-26.

Hanahan, D. 1983. Studies on transformation of *Escherichia coli* with plasmids. J. Mol. Biol. 166: 557-580.

Hanahan, D. 1985. In Glover, D.M. (ed.), *DNA Cloning Volume I: A Practical Approach.* IRL Press, Oxford, UK.

Herr, W., Chapman, N.M., and Noller, H.F. 1979. Mechanism of ribosomal subunit association: discrimination of specific sites in 16*S* RNA essential for association activity. J. Mol. Biol. 130: 433-449.

Hill, W.E., Camp, D.G., Tapprich, W.E., and Tassanakajohn, A. 1988. Probing ribosome structure and function using short oligonucleotides. Meth. in Enz. 164: 401-419.

Jacob, W., Santer, M. and Dahlberg, A.E. 1987. A single base change in the Shine-Dalgarno region of 16*S* rRNA of *Escherichia coli* affects translation of many proteins. Proc. Natl. Acad. Sci., U.S.A. 84: 4757-4761.

Kunkel, T.A. 1985. Rapid and efficient site-specific mutagenesis without phenotypic selection. Proc. Natl. Acad. Sci., U.S.A. 82: 488-492.

Lee, K., Varma, S., SantaLucia Jr., J. and Cunningham, P.R. 1997. *In vivo* determination of RNA structure-function relationships: analysis of the 790 loop in ribosomal RNA. J. Mol. Biol. 269: 732-743.

Lodmell, J.S. and Dahlberg, A.E. 1997. A conformational switch in Escherichia coli 16S ribosomal RNA during decoding of messenger RNA. Science. 277: 1262-1267.

Maniatis, T., Fritsch, E.F. and Sambrook, J. 1989. *Molecular Cloning: A Laboratory Manual.* New York: Cold Spring Harbor Laboratory Press. 1.33-1.39.

Meier, N., Goringer, H.U., Kleuvers, B., Scheibe, U., Eberle, J., Szymkowiak, C. Zacharias, M. and Wagner, R. 1986. The importance of individual nucleotides for the structure and function of rRNA molecules in *E. coli*. FEBS. 204 (1): 89-95.

Moazed, D. and Noller, H.F. 1986. Transfer RNA shields specific nucleotides in 16S ribosomal RNA from attack by chemical probes. Cell. 47: 985-994.

Moazed, D. and Noller, H.F. 1987. Interaction of antibiotics with functional sites in 16*S* ribosomal RNA. Nature. 327: 389-394.

Moazed, D. and Noller, H.F. 1989. Intermediate states in the movement of transfer RNA in the ribosome. Nature. 342: 142-148.

Moazed, D. and Noller, H.F. 1990. Binding of tRNA to the ribosomal A and P sites protects two distinct sets of nucleotides in 16*S* rRNA. J. Mol. Biol. 211: 135-145.

Moazed, D., Robertson, J.M. and Noller, H.F. 1988. Interaction of elongation factors EF-G and EF-Tu with a conserved loop in 23*S* RNA. Nature 334: 362-364.

Moazed, D., Stern, S. and Noller, H.F. 1986. Rapid chemical probing of conformation in 16*S* ribosomal RNA and 30*S* ribosomal subunits using primer extension. J. Mol. Biol. 187: 399-416.

Muralikrishna, P. and Wickstrom, E. 1989. *Escherichia coli* initiation factor 3 protein binding to 30*S* ribosomal subunits alters the accessibility of nucleotides within the conserved central region of 16*S* rRNA. Biochemistry. 28: 7505-7510.

Noller, H.F. 1991. Ribosomal RNA and translation. Ann. Rev. Biochem. 60: 191-227.

Noller, H.F., Hoffarth, V., and Zimniak, L. 1992. Unusual resistance of peptidyl transferase to protein extraction procedures. Science. 256: 1416-1419.

Noller, H.F., Moazed, D., Stern, S., Powers, T., Allen, P.N., Robertson, J.M., Weiser, B. and Triman, K. 1990. In Hill, W.E., Dahlberg, A.E., Garrett, R.A., Moore, P.B., Schlessinger, D. and Warner, J.R. (eds), *The Ribosome: Structure, Function and Evolution.* Amer. Soc. Microbiol., Washington, D.C., pp. 73-92.

Noller, H.F., Stern, S., Moazed, D., Powers, T., Svensson, P. and Changchien, L.M. 1987. Studies on the architecture and function of 16*S* rRNA. Cold Spring Harbor Symp. Quant. Biol. 52: 695-708.

Rottmann, N., Kleuvers, B. Atmadja, J. and Wagner R. 1988. Mutants with base changes at the 3'-end of the 16*S* RNA from *Escherichia coli.* Eur. J. Biochem. 177: 81-90.

Sanger, F., Nicklen, S., and Coulson, R. 1977. DNA sequencing with chain-terminating inhibitors. Proc. Natl. Acad. Sci., U.S.A. 74: 5463-5467.

Santer, M., Bennett-Guerrero, E., Byahatti, S., Czarnecki, S., O'Connell, D., Meyer, M., Khoury, J., Cheng, X., Schwartz, I., and McLaughlin, J. 1990. Base changes at position 792 of *Escherichia coli* 16*S* rRNA affect assembly of 70*S* ribosomes. Proc. Natl. Acad. Sci., U.S.A. 87: 3700-3704.

Sigmund, C.D., Ettayebi, M., Borden, A. and Morgan, E. 1988. Antibiotic resistance mutations in ribosomal RNA genes of *Escherichia coli.* Meth. in Enz. 164: 673-690.

Spirin, A.S. 1968. On the mechanism of ribosome function. The hypothesis of locking-unlocking of subparticles. Dokl. Akad. Nauk. SSSR. 179: 1467-1470.

Staplin, W.R. 1995. Thesis; University of Nebraska at Omaha. Analysis of ribosomal subunit association using mutations at position 790 of *Escherichia coli* 16*S* RNA.

Tapprich, W.E. and Hill, W.E. 1986. Involvement of bases 787-795 of *Escherichia coli* 16*S* ribosomal RNA in ribosomal subunit association. Proc. Natl. Acad. Sci., U.S.A. 83: 556-560.

Tapprich, W.E., Goringer, H.U., DeStasio, E., Prescott, C. and Dahlberg, A.E. 1990. In Hill, W.E., Dahlberg, A.E., Garrett, R.A., Moore, P.B., Schlessinger, D. and Warner, J.R. (eds), *The Ribosome: Structure, Function and Evolution.* Amer. Soc. Microbiol., Washington, D.C., pp. 236-242.

Tapprich, W.E., Goss, D.J. and Dahlberg, A.E. 1989. Mutation at position 791 in *Escherichia coli* 16*S* ribosomal RNA affects processes involved in the initiation of protein synthesis. Proc. Natl. Acad. Sci., U.S.A. 86: 4927-4931.

Vila, A., Viril-Farley, J. and Tapprich, W.E. 1994. Pseudoknot in the central domain of small subunit ribosomal RNA is essential for translation. Proc. Natl. Sci., U.S.A. 91: 11148-11152.

Wilson, K.S. and Noller, H.F. 1998a. Mapping the position of translational elongation factor EF-G in the ribosome by directed hydroxyl radical probing. Cell. 92: 131-139.

Wilson, K.S. and Noller, H.F. 1998b. Molecular movements inside the translational engine. Cell. 92: 337-349.